Riverine dissolved organic matter transformations increase with watershed area, water residence time, and Damköhler numbers in nested watersheds

Kevin A. Ryan[1*], Vanessa A. Garayburu-Caruso[2*], Byron C. Crump[3], Ted Bambakidis[3], Peter A. Raymond[4], Shaoda Liu[5], James C. Stegen[2,6]

[1]U.S. Geological Survey New York Water Science Center, Troy, New York, USA, 12180
[2]Pacific Northwest National Laboratory, Richland, Washington, USA, 99354
[3]Oregon State University, Corvallis, Oregon, USA, 97331
[4]Yale University, New Haven, Connecticut, USA, 06511
[5]School of Environment, Beijing Normal University, Beijing, China, 100875
[6] Washington State University, Pullman, WA 99163

**Correspondence to*: Kevin A. Ryan (karyan@usgs.gov)

Orcid IDs

Kevin A. Ryan, 0000-0003-1202-3616
Vanessa A. Garayburu-Caruso, 0000-0003-3383-6237
Byron C. Crump, 0000-0001-7062-1273
Ted Bambakidis, 0000-0001-8452-3500
Peter A. Raymond, 0000-0002-8564-7860
Shaoda Liu, 0000-0002-0836-5085
James C. Stegen, 0000-0001-9135-7424

Abstract. Quantifying the relative influence of factors and processes controlling riverine ecosystem function is essential to predicting future conditions under global change. Dissolved organic matter (DOM) is a fundamental component of riverine ecosystems that fuels microbial food webs, influences nutrient and light availability, and represents a significant carbon flux globally. The heterogeneous nature of DOM molecular composition and its propensity for interaction (i.e., functional diversity) can characterize riverine ecosystem function across spatiotemporal scales. To investigate fundamental drivers of DOM diversity, we collected seasonal water samples from 42 nested locations within five watersheds spanning multiple watershed sizes (~5 to 30,000 km^2) across the United States. Patterns in DOM molecular diversity and putative biochemical transformations derived from high-resolution mass spectrometry were assessed across gradients of explanatory variables associated with watershed characteristics (e.g., watershed area, water residence time, land cover). We found that putative biochemical transformations were more strongly related to explanatory variables across watersheds than common bulk DOM

parameters and that watershed area, surface water residence time and derived Damköhler numbers representing DOM reactivity timescales were strong predictors of DOM diversity. The data also indicate that catchment-specific land cover factors can significantly influence DOM diversity in diverging directions. Overall, the results highlight the importance of considering water residence time and land cover when interpreting longitudinal patterns in DOM chemistry and the continued challenge of identifying generalizable drivers that are transferable across watershed and regional scales for application in Earth system models. This work also introduces a Findable Accessible Interoperable Reusable (FAIR) dataset (>300 samples) to the community for future syntheses.

1 Introduction

Quantifying the relative influence of factors and processes controlling riverine ecosystem function is essential to predicting future conditions under global change. Dissolved organic matter (DOM) is a fundamental component of riverine ecosystems because it fuels microbial food webs, influences nutrient and light availability, and represents a significant carbon flux globally (Dittmar & Stubbins 2014; Tank et al. 2010). DOM is a complex mixture of dissolved heteroatomic organic molecules with heterogeneous molecular composition (i.e., chemical diversity) and varied propensity for interaction (i.e., functional diversity), which can be used to characterize riverine ecosystem function across spatiotemporal scales. The transport of DOM in rivers globally also forms an important component of the global carbon cycle (Tranvik et al. 2018). Thus, Earth system modelling of riverine carbon fluxes is essential for quantifying the terrestrial carbon sink (Lauerwald et al. 2020).

Along the aquatic continuum, DOM is subject to biotic and abiotic processes that alter the structure and composition of DOM, often with important biogeochemical ramifications. For example, the complete oxidation of DOM to CO_2 occurring in soil, groundwater, and surface waters contributes to significant emission of CO_2 from inland waters (up to 18% of gross primary production; Liu et al. 2022a; Raymond et al. 2013). However, a substantial quantity of DOM evades remineralization within time scales associated with terrestrial-to-marine transport (Liu et al. 2022b). This more persistent DOM is far from inert, but rather is subject to physical sorption, photo-oxidation, and microbial processing, each of which transforms DOM molecular characteristics. The chemical character of organic molecules (e.g.,

elemental composition and structure) and the surrounding aquatic matrix (e.g., solute concentration, temperature, pH, ionic strength, light, and redox conditions) influence DOM reactivity (Kaplan & Cory 2016). Accordingly, the complex nature of DOM composition and reactivity along the terrestrial-to-aquatic continuum has precluded simple representation in conceptual schematics, process-based reactive transport models, and Earth system models (Arora et al. 2022; Ward et al. 2020). Despite these challenges, understanding the processes controlling the sources, transport, and ultimate fate of DOM in river systems is essential to predicting riverine ecosystem function and carbon cycling under global change.

Vannote et al. (1980) proposed one of the earliest conceptual syntheses of riverine ecosystem function, the River Continuum Concept (RCC). The RCC posited that diversity of natural organic molecules (i.e., DOM chemical diversity) decreases from headwaters to larger rivers due to increasing biological consumption and decreasing terrestrial inputs. Since its publication, the RCC hypothesis has motivated decades of empirical study of biology and chemistry across riverine longitudinal gradients. Conceptual descendants of the RCC are based on the idea that DOM composition is determined by the balance of contributing organic carbon sources, physical removal processes, and biogeochemical transformations occurring along a downstream flow path (Bernhardt et al. 2017; McClain et al. 2003; Wollheim et al. 2018). However, all studies and syntheses are limited by the operational definitions of DOM diversity imposed by the analytical techniques available for measuring aspects of the complex DOM mixture (D'Andrilli et al. 2020). The ever-widening analytical windows of DOM chemistry has steadily increased the resolution at which DOM chemical diversity can be evaluated. Each analytical advancement has driven new insights into the nature and reactivity of DOM in natural and engineered systems (Cooper et al. 2022). Early approaches relied on elemental ratios of bulk C, N, and P and spectroscopic metrics quantifying the interaction of DOM with ultraviolet and visible light. Surpassing the limitations of bulk DOM characterization, solid-phase extraction combined with ultrahigh-resolution Fourier transform ion cyclotron resonance mass spectrometry (FTICR-MS) now commonly provides molecular-level information on DOM chemical diversity (Kujawinski et al. 2002). FTICR-MS has revealed striking diversity even in low concentrations allowing biogeochemical models, including the RCC, to be tested at unprecedented resolution (Hockaday et al. 2009; Kim et al. 2003).

Using FTICR-MS, Mosher et al. (2015) reported that 1st order, forested streams had unique molecular formula compared to higher order streams, but that overall chemical diversity persisted across the longitudinal gradient up to the 5th stream order. Thus, DOM chemical diversity cannot be assumed to decrease as merely a function of river network position. In addition, hydroclimatic and land-use factors have been shown to influence both the quantity and composition of DOM throughout the river network (Cole et al. 2007; Creed et al. 2003). Notably, Raymond et al. (2016) proposed the Pulse Shunt Concept (PSC) providing a framework for predicting the translocation of biogeochemically reactive DOM from headwaters into downstream rivers and coastal zones after hydrologic events. Conceptual frameworks that incorporate the temporal controls of watershed conditions (e.g., discharge, season) on DOM chemistry have provided important advances in understanding. However, consideration of the spatial component of river networks is equally important to assess DOM processing at the watershed scale. Surface-water residence time (WRT) has been shown to be a key hydrologic variable associated with dynamics of riverine biogeochemical constituents (Casas-Ruiz et al. 2020; Hosen et al. 2021). Derived in part from WRT and metrics of DOM loss rates over space, the Domköhler number framework can be used to quantify an advection-to-reaction timescale ratio that can indicate whether a river system is dominated by reaction versus export processes (Liu et al. 2022b). Domköhler numbers (i.e., dimensionless proxy for reaction significance) greater than 1 indicate a reaction-dominated system where reactions proceed faster than the time scale of transport through the reach, whereas values less than 1 indicate a transport-dominated system (Harvey et al. 2019; Zarnetske et al. 2012).

Numerous studies have provided evidence supporting various conceptual frameworks and their associated hydro-biogeochemical processes within watersheds (Casas-Ruiz et al. 2020; Hosen et al. 2020; Wagner et al. 2019; Wollheim et al. 2018; Yoon et al. 2021). However, descriptive studies of DOM molecular composition in small watersheds have only limited capacity to identify fundamental scaling relationships for DOM composition across catchments that vary in size, land use and geomorphology (Casas-Ruiz et al. 2020; Roebuck et al. 2020; Vaughn et al. 2021). While questions of the timing and location of DOM concentrations and loads can often be answered where empirical data are available, process-based models that omit consideration of the molecular composition of DOM are unlikely to accurately describe DOM reactivity, fate, and utility as an energy source in river networks (Arora et al.

2022). Thus, studies leveraging FTICR-MS data describing high-resolution DOM molecular properties across broad spatial scales have greater likelihood of generating novel insights concerning fundamental processes governing watershed biogeochemistry.

Functional diversity metrics applied to ecological communities quantify the variety of functional traits in an ecosystem and can indicate overall ecosystem stability (Petchey & Gaston 2006). Metrics of DOM functional diversity derived from the high dimensional data from high-resolution mass spectrometry have only recently been applied to describe DOM reactivity and stability in an ecological sense (Mentges et al. 2017; Tanentzap et al. 2019). The term "functional" here does not refer to the structural features (e.g., functional groups) of organic molecules. Instead, the term "functional" refers to the biogeochemical reactivity, and thus ecological importance, of DOM molecular formulas and compound classes. Observations of DOM composition and chemometric processing (e.g., FTICR-MS peak mass difference analysis) have shown the strong influence of external environmental conditions, microbial community composition, and metabolic capacity in predicting DOM reactivity and fate in river networks (Danczak et al. 2023; Stadler et al. 2023; Stegen et al. 2022; Stegen et al. 2018). A reduction or increase in DOC concentration does not imply a concomitant reduction or increase in DOM chemical or functional diversity (Creed et al. 2015; Hosen et al. 2020), and seemingly small changes in molecular structure and composition can alter the reactivity of DOM (Ball & Aluwihare 2014). Therefore, quantifying DOM functional diversity along longitudinal gradients in similar sized watersheds of differing geomorphology and land use is necessary to identify generalizable patterns relevant to modeling riverine ecosystem function.

Danczak et al. (2023) observed strong covariance of metrics of DOM chemical and functional diversity derived from FTICR-MS data with watershed area and land cover in the Yakima River. However, the causative factors and mechanisms driving these correlations (e.g., watershed area, land cover, hydrology) remain poorly understood. Furthermore, it is not known to what extent the patterns of organic matter diversity observed in the Yakima River are transferable to other watersheds. To further scientific understanding of the fundamental drivers of DOM diversity in river networks, we explore DOM metrics associated with seasonal water samples from 42 nested locations within five watersheds spanning multiple watershed sizes (~5 to 30,000 km^2) and stream orders (1 to 7) across the United States. We

explore relations among dependent variables that represent DOM richness (e.g., number of assigned molecular formulas), composition (e.g., aromaticity index), and functional diversity (e.g., putative biochemical transformations) derived from FTICR-MS and explanatory variables associated with watershed characteristics (e.g., watershed area, surface-water residence time, land cover). Our principal aim was to explore relations among selected dependent and explanatory variables to test specific hypotheses related to DOM composition and function within large watersheds ($>10^3$ km^2).

Assuming that the diversity of potential DOM source areas increases with increasing watershed area, we hypothesized that metrics of DOM chemical and functional diversity increase with increasing watershed area (H1). Similarly, increased surface-water residence time (WRT) increases the potential for new autochthonous contributions and further biogeochemical transformation of DOM. Thus, we hypothesized that metrics of DOM diversity increase with increasing WRT (H2). By combining the WRT with estimates of DOM uptake in a Damköhler number (Da) calculated for each sample, we further hypothesized that DOM functional diversity increases with larger Da numbers (H3). Finally, the composition of allochthonous DOM (i.e., terrestrially sourced) is influenced by the type of terrestrial organic matter represented by land-cover that is hydrologically connected to river systems and we postulate that the integration of different allochthonous DOM sources increases DOM diversity. Thus, we hypothesized that metrics of DOM diversity increase with metrics of increasing land cover diversity (H4a) and with the percent of dominant land-cover class for each watershed (H4b). Quantifying the relative variable importance among the explanatory variables was outside the scope of the current study. Future studies may combine the current data with other similar datasets and multivariate or machine learning techniques to assess explanatory variable importance.

2 Methods

To explore transferability of spatiotemporal basin-scale DOM patterns we studied DOM composition and transformations across five diverse watersheds. The study areas were selected to span a range of biomes, land-use conditions and watershed areas (Table 1 and Table S1). More information regarding site metadata can be accessed in the ESS-DIVE data packages (Otenburg et al. 2022; Torgeson et al. 2022).

2.1 Watersheds and Sample Locations

Yakima River Basin (YRB) is located in Washington state, United States. This watershed drains 15,941 km^2 and spans different ecosystems and climates from mountainous to agricultural and urban. The watershed is snowpack-driven and drains into an agricultural valley (Vano et al. 2010). This study focuses on seven sites that capture the diversity of the watershed. Each site in YRB was sampled weekly between April 2021 and October 2021 and bi-weekly (weather permitting) until April 2022 (Otenburg et al. 2022). The sites were paired with existing U.S. Geological Survey (USGS) or U.S. Bureau of Reclamation streamflow gaging stations. Sampling frequency in YRB was greater than for the other sampled watersheds because data collection in the Yakima basin was part of the routine sampling efforts for the ongoing River Corridor Science Focus Area project at Pacific Northwest National Laboratory.

The Deschutes River (DES) flows from the eastern slope of the Cascade Mountains in central Oregon, United States. The watershed drains 27,195 km^2 of land that ranges from ponderosa pine dominated headwaters to semi-arid high desert and rangeland. Like the YRB, discharge in DES is snowpack-driven. Ten sites ranging from headwaters to its confluence with the Columbia River were selected for sampling. The Willamette River (WIL) watershed lies on the opposite side of the Cascade Mountains as DES, draining the western slope and Willamette Valley in western Oregon. The watershed drains 29,008 km^2 of land ranging from forests dominated by douglas fir, western hemlock, and western red cedar at higher elevations, to agricultural and urban land in the Willamette Valley. Discharge is driven by both mountain snowpack and rainfall. The Gunnison River (GUN) watershed drains 20,533 km^2 of land in central Colorado. The basin is largely snowpack driven, with headwaters at more than 3000 m in elevation and most annual precipitation falling as snow throughout the basin. The landcover ranges from montane and coniferous forests dominated by lodgepole and ponderosa pine, aspen, and juniper. Lower elevations are comprised of mixed coniferous forest, grasslands, and rangeland. The Connecticut River (CT) watershed is the largest basin in the New England region of the United States, draining 29,070 km^2. Land cover ranges from northern hardwood-conifer mixed forest in the northern headwaters, to agricultural and urban use in the southern downstream sites. Discharge is influenced by both snowpack and rainfall. Each site in DES, WIL, GUN, and CT was sampled at least quarterly to capture conditions during all seasons (Torgeson et al. 2022). All sampling locations were at either USGS, Bureau of

Reclamation, or Oregon Water Resources Department streamflow gaging stations, or within experimental watersheds (e.g., H.J. Andrews Experimental Forest, East River Watershed Science Focus Area and Sleepers River Research Watershed).

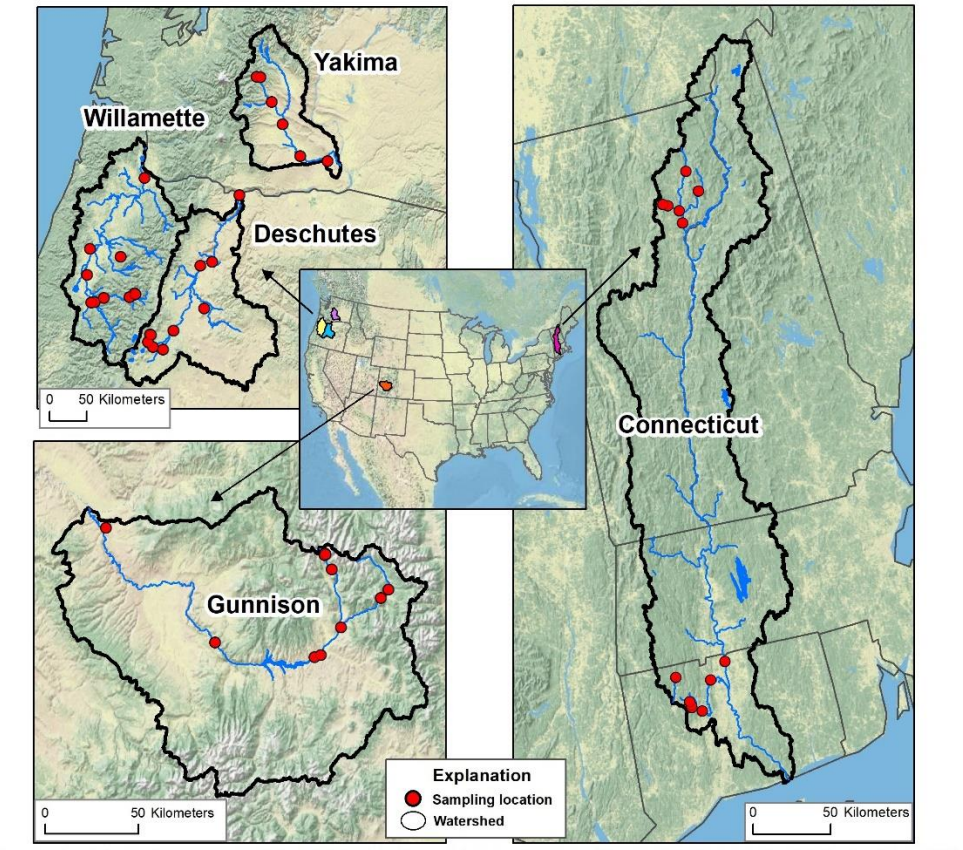

Fig 1 Map showing watershed boundaries (black) and sampling locations (red). Hydrography is shown in blue. Waterbodies less than 10 km^2 are not shown. Overlaying text refers to watershed names.

Table 1: Summary information of sample sites in the United States and ranges of stream orders, watershed areas, and elevations (datum = NAVD88) per watershed. Watershed area and elevation data are sourced

from Blodgett and Johnson (2022) and Hill et al. (2016). CT =Connecticut River, Connecticut; DES = Deschutes River, Oregon; GUN = Gunnison River watershed, Colorado; WIL = Willamette River, Oregon; YRB = Yakima River Basin. Washington state.

Watershed	Number of sites	Stream order range	Watershed area range (km^2)	Elevation range (m)
YRB	7	3-7	206-14145	880-1464
DES	10	2-6	52-25189	1002-1709
WIL	11	1-7	0.6-28922	555-1078
GUN	11	1-6	4.6-20481	2668-3507
CT	13	1-6	0.41-25009	246-570

2.2 Water Sampling

Surface-water samples were collected at each location for measurements of non-purgeable dissolved organic carbon (DOC) and for ultrahigh-resolution mass spectrometry measurements. DOC samples from YRB were collected in triplicate using 60 mL sterile plastic syringes, and singly from DES, WIL, GUN and CT using a peristaltic pump with acid-cleaned tubing. DOC samples were immediately filtered through a 0.22 μm sterivex filter (EMD Millipore), transported on ice in non-acidified 40 mL glass vials (YRB; I-Chem amber VOA glass vials; ThermoFisher) or 60 mL polycarbonate bottles (DES, WIL, GUN, CT) and stored refrigerated until analysis at Pacific Northwest National Laboratory (PNNL, YRB) or Yale University (DES, WIL, GUN, CT). Samples for ultrahigh-resolution mass spectrometry were collected in triplicate at all sites with 60 mL syringes, filtered through sterivex filters into 40 mL glass vials with 10 μL of 85% phosphoric acid, shipped to PNNL and placed in a -20 °C freezer.

2.3 Chemical analyses

Dissolved organic carbon as non-purgeable organic carbon was analyzed within 2 months of sample collection using non-acidified filtered samples. Samples were stored in the dark at 6°C until analysis. DOC in YRB samples was measured at PNNL by sparging 150 µL of sample into a Shimadzu TOC-L Total Organic Carbon Analyzer connected to an ASI-L autosampler and then selecting the average of the best 3 out of 5 injections to get a final concentration. The DOC calibration curve spanned 0.25 to 100 mg C L^{-1}. Concentrations below the limit of detection of the instrument, or below the standard curve were flagged. DOC in DES, WIL, GUN, and CT samples was measured at the Yale University Raymond Lab following Hosen et al. (2021a), in which samples were acidified to 2% of 2 M HCl, sparged for 5 min., and measured on a Shimadzu Total Organic Carbon Analyzer (TOC-vCPH with TNM-1, Shimadzu Corporation, Kyoto, Japan). The DOC results from this section were used to prepare samples for FTICR-MS, described in the section below.

2.4 FTICR-MS analysis

Surface-water samples were analyzed using ultrahigh-resolution mass spectrometry techniques following Garayburu-Caruso et al. (2020). Briefly, samples collected in pre-acidified glass vials were thawed in the dark at 4 °C for 72 h. Samples were diluted to 1.5 mg C L^{-1}, based on the water sample DOC concentrations. Samples were acidified to pH 2 with 85% phosphoric acid before proceeding into solid phase extraction protocol, where 15 mL were loaded onto preconditioned PPL cartridges (Bond Elut), dried under positive pressure and eluted with 1.5 mL of methanol (Dittmar et al. 2008).

We used a 12 Tesla (12 T) Bruker SolariX Fourier transform ion cyclotron mass spectrometer (FTICR-MS; Bruker, SolariX, Billerica, MA, USA) located at the Environmental Molecular Sciences Laboratory in Richland, WA to analyze samples post solid phase extraction. Ultrahigh-resolution spectra were acquired in negative mode using an electrospray ionization source. Samples were run in separate batches where the resolution was 256 K for YRB samples and 385 K at 481.185 m/z for all other samples. The voltage was set to +4.5 kV. The instrument was calibrated weekly, and settings were optimized using a Suwannee River Fulvic Acid standard. Data were collected with ion accumulations of 0.08 to 0.1 from

100 to 900 m/z at 4 M. One hundred forty-four scans were co-added for each sample and internally calibrated using an OM homologous series separated by 14 Daltons (–CH2 groups). The mass measurement accuracy was typically within 1 ppm for singly charged ions across a broad m/z range (100 m/z–900 m/z).

Raw spectra were converted to a list of m/z using BrukerDaltonik Data Analysis (version 5.0). Further an FTMS peak picker module with a signal-to-noise ratio of 7 and absolute intensity threshold to the default value of 100 was applied and peaks were aligned using a 0.5 ppm threshold. We used Formularity along with the Compound Identification Algorithm (Tolic et al., 2017) to assign chemical formulas by only taking into consideration the presence of C, H, O, N, S, and P and using S/N > 7 and mass measurement error <0.5 ppm. We removed peaks outside of a high confidence m/z range (200 m/z–900 m/z) and/or with a ^{13}C isotopic signature, calculated molecular formula properties and assigned metabolites to chemical classes based on their oxygen-to-carbon and hydrogen-to-carbon ratios using R package "ftmsRanalysis" (Bramer et al. 2020; R Core Team 2023). The modified aromaticity index was calculated according to Koch and Dittmar (2006). The relative abundance of molecular formulas containing specific elemental composition (e.g., CHON, % RA) was calculated by normalizing by the total number of molecular formula assigned within a given sample.

2.5 Putative biochemical transformation analysis

We inferred biochemical transformations from ultrahigh-resolution mass spectrometry data following Garayburu-Caruso et al. (2020) and Danczak et al. (2023). Spectra from sample replicates were combined such that peaks were considered only if they were present in at least one of the three replicates producing a single composite spectrum for each sample. Peak intensities were changed to binary presence/absence where masses with a value of "0" indicate the peak was removed because it did not meet the replicate presence requirements and a value of "1" indicates the peak was kept. Putative biochemical transformations were estimated by calculating the pairwise mass difference between every peak present in a sample. These differences were compared to a library of common transformation masses (n = 1,255). If the pairwise mass differences matched the masses in the reference list within 1 ppm of error, then we inferred the gain or loss of that compound via a biochemical transformation. For example,

if the mass peak between two peaks corresponded to 57.02146, that would match the reference library to the gain or loss of glycine. For comparison across samples with different DOM number of peaks, the number of transformations was normalized to the number of peaks present in that sample (Norm. Trans.).

2.6 Geospatial data

Geospatial data was extracted for each site using a custom R script (Willi & Ross 2023). Each site's watershed was delineated with the R package 'nhdplusTools' (Blodgett & Johnson 2022) and key National Hydrography Dataset Plus (NHDPlus V2) variables were extracted (e.g., catchment area). Sites located on water bodies too small to be captured by the NHDPlus do not have watershed metrics but key variables for the analysis performed in this manuscript were extracted from previous studies (Johnson et al. 2021; Shanley et al. 2015). Additional environmental variables from each site's watershed were extracted from the Environmental Protection Agency's StreamCat Dataset (Hill et al. 2016).

An index of biological diversity was adapted to assess the similarity of the proportion of land use and land cover (LULC) types contributing to each sample site using the proportion of each land use or land cover class (p_i) and the total number of classes (S) (Pielou 1966).

$$LULC\ Evenness = \frac{-\sum p_i \times \ln p_i}{\ln S} \quad \text{(Equation 1)}$$

The LULC classes included in the LULC evenness index were: % open water, % mixed forest, % deciduous forest, % coniferous forest, % crop land use, % woody wetland cover, % herbaceous wetland cover, % high intensity urban development, and mean % impervious land cover. Greater values of the LULC evenness index indicate increased diversity of contributing land use and more even abundances of different contributing land use classes.

2.7 Surface water residence time

Estimates for surface water residence time (WRT) followed the general procedure described in Liu et al. (2022b). Briefly, WRT estimates were based on the GRADES (Global Reach-Level A Priori Discharge Estimates for SWOT) river networks (Lin et al. 2019). We delineated the watershed

corresponding to each sampling site, by identifying all associated upstream flowlines and unit catchment areas using topological relationships describing connectivity of all GRADES flow lines. We used the mean daily discharge at each sampling station and on each sampling day to estimate sample-specific WRTs. Mean daily discharge values were acquired from the U.S. Geological Survey National Water Information System (U.S. Geological Survey 2016) or the Oregon Water Resources Department Near Real Time Hydrographics Data (https://apps.wrd.state.or.us/apps/sw/hydro_near_real_time/). Discharge data from gages operated in cooperation with the U.S. Bureau of Reclamation were also sourced from the USGS. WRT at a single river reach was calculated as length (*m*) divided by flow velocity (m s^{-1}). Flow velocity was computed using a hydraulic geometry formulation of Manning's equation using a rectangular river channel (Dingman 2007) (Eq. 2):

$$V = \left(\frac{S^{0.3}}{n^{0.6} W_b^{0.4}}\right) Q^{0.4} \quad \text{(Equation 2)}$$

where *V* is flow velocity (m s^{-1}), S is channel slope (unitless), W_b (m) is bankfull reach width, and Q (m^3 s^{-1}) is mean daily discharge. Bankfull widths were acquired from Lin et al. (2020). A uniform Manning's *n* of 0.03 was assumed.

Accumulated WRT at the sample site was estimated by routing reach-level WRTs through the delineated upstream watershed for the sampling site. We employed a discharge-weighted algorithm for routing where cumulative WRTs from all joining upstream reaches were weighted by their respective reach discharge, plus the independently estimated (i.e. reach length divided by flow velocity) advection time at the downstream reach, to obtain an average, cumulative WRT at the downstream reach (Hosen et al. 2021) (Eq. 3):

$$t_{ri} = \frac{\sum Q_j t_{rj}}{\sum Q_j} + t_i \quad \text{(Equation 3)}$$

where t_{ri} and t_{rj} (hr) were cumulative WRTs at the downstream reach *i* and the *j*th joining reach, respectively; Q_j was water discharge at the *j*th joining reach (m^3 s^{-1}); and t_i was the advection time at the single downstream reach *i*.

Dams or reservoirs from the HydroLakes database (Messager et al. 2016) were joined into the GRADES river networks. The HydroLakes database provided annual WRT estimates for each included single reservoir, which was calculated from statistically modeled reservoir volumes and outflow discharge. To estimate reservoir contribution to river network WRTs at the annual timescale, we replaced WRT at natural GRADES river reaches where HydroLakes reservoirs are situated with HydroLakes reservoir residence times for the river network scale routing. Reservoir WRT was calculated as the difference between the routed WRT with reservoir contribution and without. Reservoir contribution to river network WRT was only estimated at the annual timescale, considering only annual reservoir WRTs were available from HydroLakes (Messager et al., 2016).

Given the GRADES river networks minimum watershed area of 25 km^2, several headwater sampling sites in this study are not included in the GRADES database. To estimate WRT for these headwater sites, we fit scaling models for each watershed. Using all downstream sites >25 km^2 that were in the GRADES database, we regressed the log10 product of mean daily discharge and watershed area against the log10 of WRT. We then constructed linear best-fit equations and subsequently estimated headwater site WRTs from these watershed-specific equations, using upstream area acquired from the higher-resolution NHDPlusHR.

2.8 Damköhler number calculation

Dimensionless Damköhler numbers (Da) for each sample were calculated as the ratio between the surface water residence time (WRT, h) and a temperature-dependent aquatic DOC uptake velocity representing a characteristic reaction time following Liu et al. (2022b),

$$Da = \frac{WRT/24}{d/v_f} \text{ (Equation 4)}$$

where d is the discharge weighted mean reach water column depth (m) of river segments within the upstream watershed and v_f is the DOC uptake velocity (m d^{-1}) (Eq. 4). Uptake velocity was scaled with in-situ water temperature according to the Arrhenius law (Liu et al. 2022b). The v_f at the reference temperature (0.038 m d^{-1} at 15°C) was selected from the Ipswich River, USA reported in Wollheim et al. (2015). Da can be used to quantify the relative influence of transport versus reaction processes controlling

DOM concentrations in a river network where a Da greater 1 indicates a reaction-dominated system and a Da less than 1 indicates an export-dominated system (Gootman et al. 2020; Harvey et al. 2019).

2.9 Data Analysis

Statistical summaries were completed using the 'rstatix' R package (Kassambara 2020). The explanatory variables that ranged greater than 2 orders of magnitude (watershed area, WRT, Da) were log transformed to satisfy assumptions of normal distribution. To ascertain the general strength and direction of relations among dependent and explanatory variables, Pearson's correlation coefficients (r) and coefficients of determination (r^2) were calculated for each variable pair and for each watershed. A p-value of 0.1 was used to indicate significance. Correlation coefficients (r) are reported in the text and figures only when $p < 0.1$. Models were fit using mean variables of each sample site.

3 Results and Discussion

Table 2 Number of samples (n), mean ($\bar{x}$) and standard deviation (s.d.) for dependent variables dissolved organic carbon (DOC), the number of Fourier transform ion cyclotron resonance mass spectrometry (FTICR-MS) peaks with assigned formula (Richness), the modified aromaticity index (AI_mod), relative abundance of carbon, hydrogen, oxygen, nitrogen (CHON) formulas (CHON, % RA), and the normalized putative biochemical transformations (Norm. Trans.).

Watershed	n	DOC		Richness		AI_mod		CHON		Norm. Trans.	
		mg-C L^{-1}						% RA			
		$\bar{x}$	s.d.	$\bar{x}$	s.d.	$\bar{x}$	s.d.	$\bar{x}$	s.d.	$\bar{x}$	s.d.
Yakima	193	1.38	0.49	5167	444	0.24	0.02	12.2%	2.5%	10.5	0.6
Deschutes	43	1.01	0.92	2716	893	0.18	0.04	8.8%	3.1%	9.9	1.7
Willamette	52	1.25	0.44	3504	736	0.21	0.02	8.7%	2.2%	11.1	1.1
Gunnison	29	1.51	1.11	3515	1080	0.22	0.03	10.8%	2.6%	10.5	1.7
Connecticut	45	2.89	1.26	3970	836	0.23	0.03	10.3%	2.0%	11.0	1.5

3.1 Covariance between DOM chemistry and explanatory variables

Sampling in the Yakima was completed weekly or bi-weekly for each site, while one sample per season was targeted for other watersheds. As a result, samples from sites within the Yakima basin (n = 193) comprised ~50% of samples in the dataset. Any assessment of results for all watersheds combined are skewed toward characteristics of the Yakima samples and therefore our analysis maintains separation of samples by watershed. Mean DOC concentration for individual watersheds (range: 1.0 to 2.9 mg-C L^{-1}) was lower than the average concentration for rivers surveyed across the United States (between 2 to 10 mg-C L-1; Spencer et al. 2012). Logistical constraints on the timing of sampling may have limited sampling peak concentrations of DOC in rivers which are generally known to exceed 10 mg-C L^{-1} during individual hydrologic events.

Molecular aromaticity, as indicated by the modified aromaticity index, was similar across all watersheds (0.22 ± 0.03), however, these values were lower than peak abundance-weighted AI_{mod} values observed in samples throughout a 36,000 km^2 watershed in Georgia, USA (AImod > 0.3; Roebuck et al. 2020), throughout a 1,124 km^2 watershed in New England, USA (mean AI_{mod} = 0.3; Wagner et al. 2019) and in the upper Mississippi watershed (AI_{mod} > 0.3; Vaughn et al. 2021). DOM richness, as indicated by the number of assigned formulas to FTICR-MS peak data, was notably higher in the Yakima samples (mean = 5,167; s.d. = 444) than all other samples combined (3,426 ± 886; Table 2; Fig. S1). The number of assigned molecular formulas containing C, H, O, and N, (CHON) an indicator of potentially reactive dissolved organic nitrogen (DON), ranged from 42 to 948 formulas (mean = 405) across all watersheds. To aid in comparisons across watersheds, the number of CHON formulas are normalized to the total number of assigned formulas in a sample (CHON, % RA). Percent relative abundance of CHON ranged from 3.4 to 18 % of assigned formulas which is lower than the % formula relative abundance reported from varied land use in the Upper Mississippi River, USA (~18%; Vaughn et al. 2021) and for rivers globally (>30%; Wagner et al. 2015).

Although all samples from all watersheds were processed using standardized procedures in the same laboratory and instrument for FTICR-MS data, and were processed together in Formularity, they were analyzed in separate instrument batches. The analysis batch containing the Yakima samples had a higher mass spectrum resolution which likely contributed to a greater number of detected peaks and putative

biochemical transformations detected in those samples compared to other watersheds. The number of assigned molecular formulas used in FTICR-MS analyses never exceeds the number of detected mass peaks and depends on the processing steps taken by each investigation. Thus, molecular richness as indicated by the number of assigned formulas is not directly comparable among studies, although the reporting of thousands (> 3,000) of detected molecular peaks and % relative abundance is common (Hawkes et al. 2020). However, despite the potential for interference due to instrument variability, the values of putative biochemical transformations normalized to the number of observed mass peaks in each sample were also similar across all watersheds (10.6 ± 1.3) and the total number of transformations observed (~8,000 to 80,000) overlaps within the range reported for surface waters spanning the contiguous United States (~10,000 to 50,000; Stegen et al. 2022). Interpreting patterns of FTICR-MS metrics (e.g., transformations) across gradients of explanatory variables (e.g., watershed size) can improve understanding of ecological drivers despite the limitations common to FTICR-MS methodologies.

Although the seasonal sampling of the study design provided broader representation of annual watershed conditions, no clear pattern of DOC concentration or DOM composition emerged across winter, spring, summer, and fall seasons assigned for each region (Fig. S2). Thus, season was excluded as a supplemental explanatory variable for these data. Assessment of relations among five dependent variables and six explanatory variables across five watersheds yielded 150 individual covariance results. Linear models for log-transformed explanatory variables watershed area, WRT, and Da indicated 32 variable pairs with significant covariance ($p < 0.1$). Linear models for non-transformed land use and land cover explanatory variables indicated 26 variable pairs with significant linear covariance.

No clear pattern of DOC concentration was observed across gradients of watershed area, WRT, or Da (Figs 2, 3, and 4). Although nearly all linear fit lines had positive slopes, the Gunnison watershed was the only watershed with statistically significant covariance ($r > 0.7$; $p < 0.01$) between DOC concentration and watershed area and WRT. DOC significantly increased with Da in the Gunnison and the Yakima watersheds (Fig. 4). Other studies have reported both increases in DOC yield at higher stream orders and chemostatic behavior (i.e., stable concentrations across a broad range of conditions) with increasing watershed size (Creed et al. 2015; Hosen et al. 2020). These results suggest that DOC in the

higher order rivers in this study represents an integration of DOC from the increased supply of carbon sources across the watersheds. In support of this broad interpretation are the increasing patterns of DOC concentrations with increasing LULC evenness (Fig 5) and decreasing DOC concentration with increasing % coniferous land cover in the Willamette watershed (Fig S3; $r < -0.5$) and with increasing % deciduous cover in the Connecticut watershed (Fig. S4). The lack of a universal pattern in DOC concentration could be considered consistent with the myriad processes influencing aquatic organic matter from degradation and decomposition to autochthonous production and transformation across the terrestrial-aquatic continuum (Hedges et al. 2000; Kaplan & Cory 2016).

Similar to DOC concentration, aromaticity index was not significantly related to watershed size, WRT, nor Da except in the Gunnison watershed ($r > 0.5$), however, there was no evidence of decreasing aromaticity with these explanatory variables for all watersheds. These results contrast somewhat with Creed et al. (2015) who reported a decrease in DOM aromaticity with increasing stream order using an optical index, specific ultraviolet absorbance ($SUVA_{254}$), at 200 sites within the USA. Higher $SUVA_{254}$ values indicate higher absorbance per unit carbon due generally to increased aromaticity of the dissolved organic matter commonly observed in wetlands and headwater streams (D'Andrilli et al. 2022). Similarly, there was no clear association between AI_{mod} and LULC evenness, although positive linear covariance was apparent in the Connecticut ($r > 0.5$) and Deschutes watersheds (Fig 5). Notably, covariance between aromaticity index and % coniferous land cover was significantly positive in the Gunnison watershed (Fig S3; $r > 0.7$) and negative in the Deschutes watershed ($r < -0.7$) although patterns for % deciduous land cover were less clear (Fig. S4). In contrast to the patterns of DOC, richness, and AI_{mod}, the relative abundance of CHON formulas showed strong positive covariance with watershed area, WRT, and Da with the notable exception in the Deschutes watershed which contained one outlier sample site (Table S1; TRO-GAT). CHON formulas also strongly increased with LULC diversity in some watersheds (Fig. 4) but decreased with % coniferous land cover (Fig. S3). We interpret increases in the relative abundance of N-containing DOM as an indicator of increased DOM bioavailability (Vaughn et al. 2023) and/or increased anthropogenic inputs (Wagner et al. 2015).

The assessment of covariance of DOM chemical and functional diversity metrics with explanatory variables showed variability across watersheds similar to that of DOC and aromaticity. However, of all

dependent variables, normalized putative biochemical transformations had the highest number of significant relations (17) across watersheds and explanatory variables (see discussion below). These general results are consistent with previous studies indicating that chemometric processing of DOM molecular formulas through mass difference analyses can be good indicators of the strong influence of external environmental conditions, microbial community composition, and other factors influencing DOM reactivity and fate in river networks (Danczak et al. 2023; Stegen et al. 2022). Further detailed discussion of the covariance of DOM richness and functional diversity with explanatory variables is structured by the study hypotheses in section 3.2. Overall, no single dependent variable (e.g., DOC, aromaticity index, etc.) co-varied with all explanatory variables (e.g., watershed size, WRT) in the same direction or the same magnitude and all significant covariance was in the positive direction except for increasing % coniferous and deciduous land cover for some watersheds.

3.2 Hypotheses of DOM diversity patterns with explanatory variables

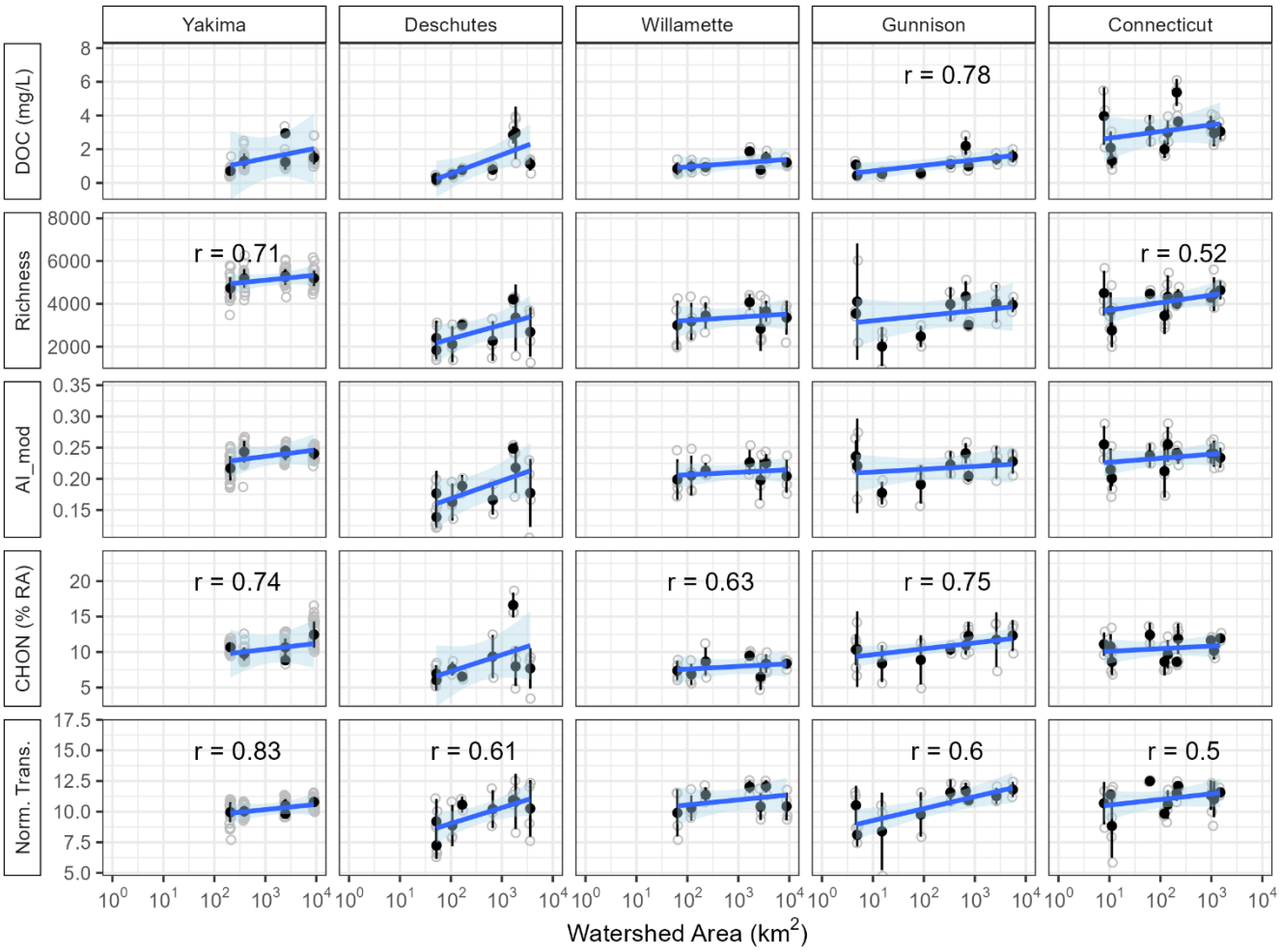

Fig 2 Dependent variables dissolved organic carbon (DOC) concentration, number of assigned formulas (Richness), modified aromaticity index (AI_mod), the percent relative abundance of assigned molecular formula containing carbon, hydrogen, oxygen, and nitrogen (C, H, O, and N) normalized to the total number of formula (CHON, % RA), and the total number of putative biochemical transformations normalized by number of peaks (Norm. Trans.) versus the logarithm (base 10) of watershed area for each watershed. Solid black points and error bars represent the mean and standard deviation of a sample site.

485 Open grey circles represent all data. Linear regression line of best fit is shown in blue and 95% confidence
486 interval is shown in light blue. Correlation coefficients (r) are shown when $p < 0.1$
487
488 We hypothesized that metrics of DOM chemical and functional diversity would increase with
489 increasing watershed area (H1). We assume that watershed area is one proxy of the heterogeneity of
490 landforms and carbon sources within a watershed and that DOM diversity in streamwater is an integrated
491 signal from these landscapes. Thus, the diversity of potential DOM sources and opportunities for
492 molecular transformation are hypothesized to increase with watershed area. Our results do not indicate a
493 clear trend of decreasing DOM richness with increasing watershed area, although significant positive
494 covariance was observed for the Yakima and Connecticut watersheds (Fig 2; $r > 0.5$). Casas-Ruiz et al.
495 (2020) used generalized additive models to determine that watershed area was a good predictor of solid
496 phase extracted DOM molecular formula richness in sites throughout a 6^{th} order stream watershed in the
497 Iberian Peninsula. That study suggested both an increase in DOM richness from the headwaters ($< 10^2$
498 km^2) to larger rivers ($\sim 10^3$ km^2) especially at higher flows, and a decreased DOM richness with the largest
499 watershed area, especially during lower flows.
500 The River Continuum Concept predicted that DOM chemical diversity decreases by ~60% between
501 first and third order streams and continues to steadily decrease longitudinally in higher order rivers
502 (Vannote et al. 1980). More recent studies employing high resolution mass spectrometry have shown that
503 DOM chemical diversity in temperate rivers is only reduced by 20-25% between first and second order
504 streams, with varying but minimal changes among higher order streams (Mosher et al. 2015). In a
505 Mediterranean river, the DOM chemical diversity was highest in mid-sized catchments relative to both
506 headwaters and higher order stream (Casas-Ruiz et al. 2020). In a tributary of the Connecticut River,
507 DOM chemical diversity did not vary significantly among stream orders (Wagner et al. 2019). Since our
508 knowledge of DOM sources, composition, and reactivity has deepened since the RCC was first proposed,
509 we now understand that geomorphic features (e.g., wetlands) and autochthonous inputs (e.g., from
510 phytoplankton) can greatly influence riverine DOM diversity (Inamdar et al. 2012; Roebuck et al. 2020).
511 Taken together, these longitudinal trends indicate that an exponential decrease in DOM chemical diversity
512 postulated in the RCC cannot be assumed, which has important implications for scaling and predictive

513 modeling of DOM export. In addition, identifying generalizable conclusions about the functional activity
514 of DOM across watershed scales allows process-based models to more accurately integrate ecological hot
515 spots, hot moments, and control points that yield outsized influence on biogeochemical processes
516 (Bernhardt et al. 2017; McClain et al. 2003).

517 Linear-log models between normalized transformations and increasing watershed area were
518 significantly positive for all watersheds except the Willamette (Fig 2). Danczak et al. (2023) reported a
519 stronger linear correlation ($R^2 = 0.93$; $p < 0.01$) for the same sites in the Yakima watershed. However,
520 watershed area in Danczak et al. (2023) was not log-transformed and fewer samples (< 50 samples across
521 6 sites) were available for analysis in the earlier study. Our study included a full year of samples and a
522 broader range of hydrologic and seasonal conditions. Thus, the reduced strength of the covariance in this
523 study may reflect an increased influence of environmental variability across the broader sample set.
524 Despite differences in the magnitude among rivers, these results suggest a strong relation between the
525 degree of putative biogeochemical processing and increasing watershed area is consistent over time. The
526 positive covariance of bulk DOM composition and metrics of molecular diversity with watershed area
527 suggests relative catchment position is associated with watershed features that increase DOM diversity,
528 although the strength of this pattern is expected to vary among watersheds and may not be universally
529 applicable.

530 Upstream watershed area is often a useful proxy for annual discharge, but it does not capture seasonal
531 and interannual variability in discharge nor the impact of that discharge on DOM processing in rivers.
532 Hydrology and season are inextricably linked in our temperate study watersheds where discharge is
533 typically highest during spring and late fall driven by storms and/or snowmelt and lowest during late
534 summer and early fall. As with most watersheds in the USA, all the watersheds in the current study contain
535 reservoirs. However, the spatial organization of these reservoirs within the watersheds vary. For example,
536 the Deschutes and Gunnison Rivers have large reservoirs on the mainstem that receive water from the
537 entire upstream watershed. In contrast, the Connecticut, Willamette, and Yakima Rivers do not have
538 significant mainstem reservoirs near the outlets, but they do have reservoirs associated with the lower
539 order tributaries. WRTs calculated for samples in the Yakima watershed were more constrained (range =

16 to 226 h) than for the other four watersheds (range = 1 to 28,000 h), potentially due to differences in dam density (range 0 to 0.07 dams km^{-2}).

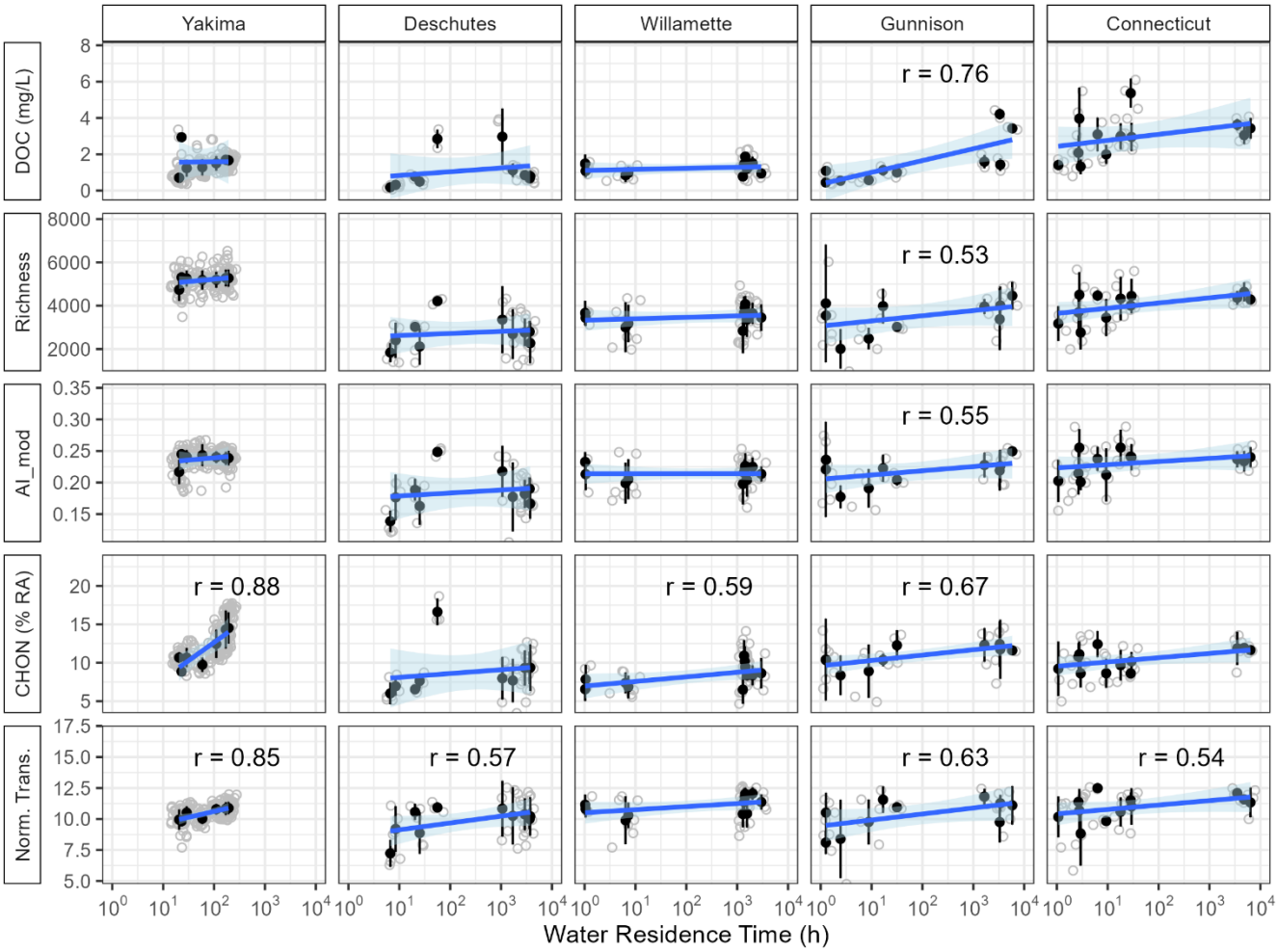

Fig 3 Dependent variables dissolved organic carbon (DOC) concentration, number of assigned formulas (Richness), modified aromaticity index (AI_mod), the percent relative abundance of assigned molecular formula containing carbon, hydrogen, oxygen, and nitrogen (C, H, O, and N) normalized to the total number of formula (CHON, % RA), and the total number of putative biochemical transformations normalized by number of peaks (Norm. Trans.) versus the logarithm (base 10) of the surface water residence time (WRT) for each watershed. Solid black points and error bars represent the mean and

standard deviation of dependent variables and WRT for each sample site. Open grey circles represent all data. Linear regression line of best fit is shown in blue and 95% confidence interval is shown in light blue. Correlation coefficients (r) are shown when $p < 0.1$

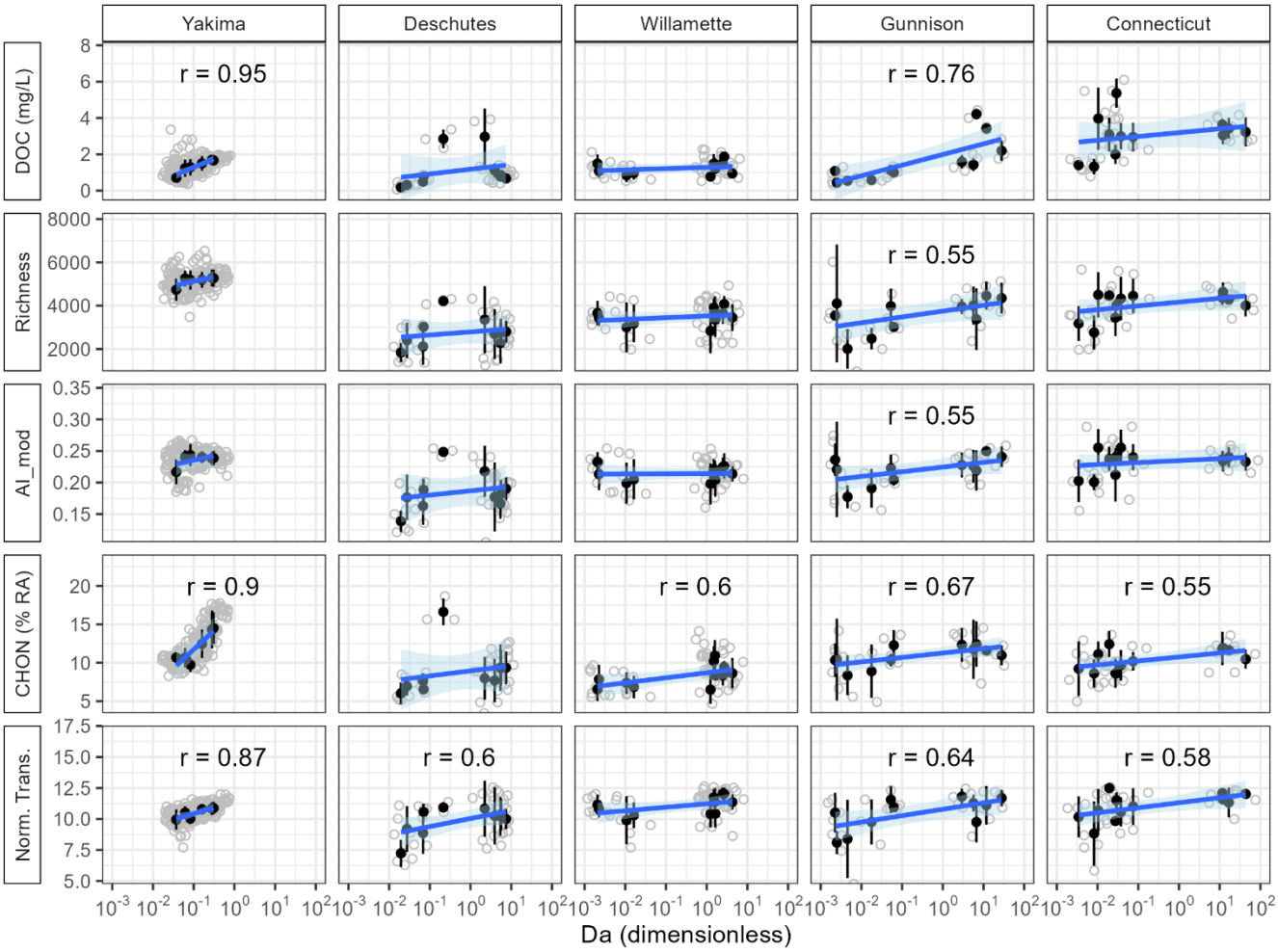

Fig 4 Dependent variables dissolved organic carbon (DOC) concentration, number of assigned formulas (Richness), modified aromaticity index (AI_mod), the percent relative abundance of assigned molecular formula containing carbon, hydrogen, oxygen, and nitrogen (C, H, O, and N) normalized to the total number of formula (CHON, % RA), and the total number of putative biochemical transformations normalized by number of peaks (Norm. Trans.) versus the logarithm (base 10) of the Damköhler number (Da) for each watershed. Solid black points and error bars represent the mean and standard deviation of

dependent variables and Da for each sample site. Open grey circles represent all data. Linear regression line of best fit is shown in blue and 95% confidence interval is shown in light blue. Correlation coefficients (r) are shown when $p < 0.1$

We hypothesized that metrics of DOM diversity would increase with increasing surface WRT (H2) and Da (H3) due to increased autochthonous DOM production and increased opportunity for biogeochemical transformations within the river network (Hosen et al. 2021; Liu et al. 2022b). Patterns of DOM richness and normalized transformations with increasing WRT across watersheds were similar to patterns described above for watershed area. However, watershed area does not scale consistently with WRT because of variation in riverbed morphology and reservoir distribution, and seasonal variation in discharge. Dimensionless Da calculated for individual samples ranged from 0.001 to 75 which spans the range of Da numbers calculated for global rivers (from <0.001 to >90; Liu et al. 2022b). Da was generally larger for higher order streams and lowest for headwater sites. Significant covariance between DOM richness and WRT or Da was observed only for the Gunnison watershed. The lack of clear trends across all watersheds could be interpreted as chemostatic behavior arising from the varying dominance of supply, transport, and reactivity controls within broadly sampled river systems (Creed et al. 2015). In contrast, linear-log models between normalized putative biochemical transformations and increasing WRT and Da were significantly positive for all watersheds except the Willamette watershed (Fig 3 & 4; $0.54 < r < 0.87$). In addition, significant positive covariance between normalized transformations and WRT and Da was strongest in the Yakima watershed, suggesting that although reservoirs increase WRT, the scaling of DOM functional metrics across watersheds may be most robust for watersheds with fewer large dams. Mean dam density for all Yakima sampling sites (0.0015 dams km^{-2}) was lower than that of all other sites (0.007 dams km^{-2}).

Previous studies have shown that threshold points in river systems related to WRT may exist in which the composition of in-stream DOM becomes disconnected from upstream and lateral sources and instead reflects local inputs and microbial-mediated processes (Coble et al. 2022; Hosen et al. 2021). Therefore, a zone of inflection in DOM composition and reactivity could be expected to occur at the transition between allochthonous versus autochthonous control. The linear-log relations detected in the dependent

variables across watershed area and WRT is consistent with such an inflection point in mid-sized river reaches. Accordingly, Liu et al. (2022b) found that DOC uptake in global river networks becomes more reaction-dominated (i.e., autochthonously controlled) at the transition between 5th and 6th order streams. In addition, DOM composition can vary substantially more with discharge than with stream order (Wagner et al. 2019), highlighting how individual hydrologic events alter DOM composition and reactive potential that is normally present during low flow conditions. Thus, the location of any transition point would be dependent on flow conditions (Raymond et al. 2016). Overall, our results suggest that WRT and Da are associated with mechanisms across basins that increase DOM functional diversity across broad flow regimes and watershed morphology.

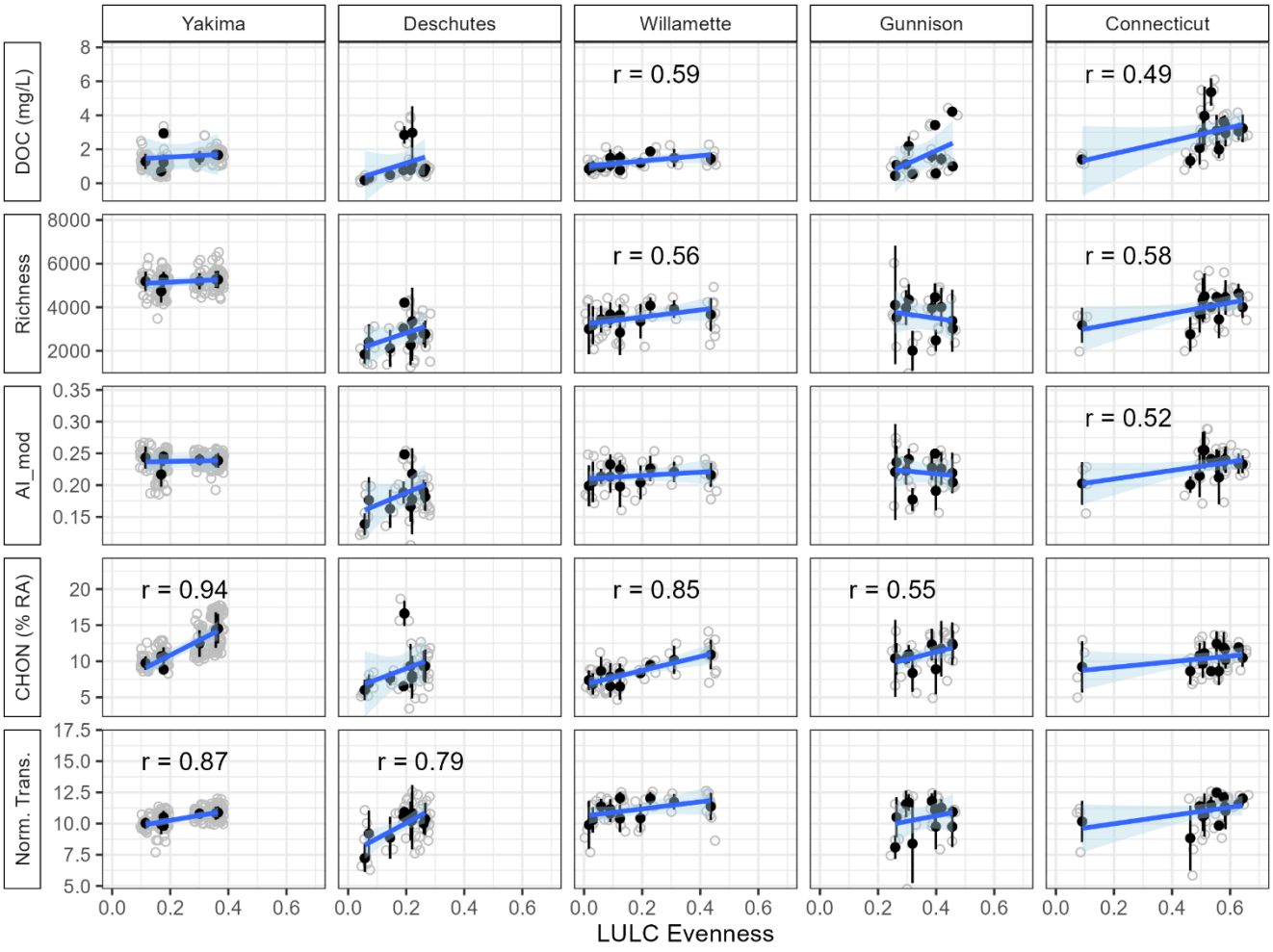

Fig 5 Dependent variables dissolved organic carbon (DOC) concentration, number of assigned formulas (Richness), modified aromaticity index (AI_mod), the percent relative abundance of assigned molecular formula containing carbon, hydrogen, oxygen, and nitrogen (C, H, O, and N) normalized to the total number of formula (CHON, % RA), and the total number of putative biochemical transformations normalized by number of peaks (Norm. Trans.) versus an index of land use and land cover (LULC) for each watershed (Eq. 3). Solid black points and error bars represent the mean and standard deviation of a sample site. Open grey circles represent all data. Linear regression line of best fit is shown in blue and 95% confidence interval is shown in light blue. Correlation coefficients (r) are shown when $p < 0.1$

We hypothesized that metrics of DOM diversity would increase with increasing land-cover diversity (H4a) and with the percent of dominant land-cover class for each watershed (H4b). The composition of allochthonous DOM is influenced by the type of terrestrial organic matter that is hydrologically connected to river systems whereby the integration of different allochthonous DOM sources increases DOM diversity. We estimated contributing organic matter source diversity using an index of land-cover diversity (LULC evenness; Equation 1) where higher evenness represents a greater number of land use classes contributing in similar proportions to a given sample site. DOM richness increased significantly with increasing LULC evenness in the Willamette and Connecticut watersheds (Fig 5; $r > 0.5$) while patterns for the other three watersheds were less clear. Putative biochemical transformations increased significantly with increasing LULC evenness in the Yakima ($r = 0.87$) and Deschutes watersheds ($r = 0.79$), while nonsignificant increasing patterns were observed for the other three watersheds. No pattern in any watershed indicated any decreasing trend of biochemical transformations with increasing LULC evenness. The range of LULC evenness varied across watersheds and most sites in the Connecticut watershed had greater evenness (> 0.4) than all other watersheds. The similar ecosystems and physical geography within the Yakima and Deschutes watersheds may provide some explanation for similarities in patterns of DOM functional diversity with changes in land use and land cover.

Due to the extensive connectivity between surface waters and the landscapes they drain, land cover and land use type can be more important controls on DOM composition than stream order (Coble et al.

2022; Roebuck et al. 2020). Vaughn et al. (2021) reported positive relations between DOM molecular formula associated with terrestrial allochthonous sources (e.g., aromatic, polyphenolic compounds) and percent forest cover in the Upper Mississippi watershed, and showed that multivariate indices of molecular composition were distinct among samples from primarily forest, agriculture, and urban sites throughout all seasons. Roebuck et al. (2020) used redundancy analysis to show that dominant land-use class explained ~50% of DOM composition, characterized using optical and FTICR-MS indices, across a large watershed in the southeast USA, while stream order explained only less than 10% of the variance. Human activities such as agriculture and urbanization are known to alter DOM composition in inland waters (Xenopoulos et al. 2021). DOM exported by anthropogenically impacted catchments has a different ecological and biogeochemical fate than DOM exported by predominantly forested catchments, even if bulk DOC concentrations are comparable (Roebuck et al. 2020; Vaughn et al. 2021; Wagner et al. 2015). Although the contributing relative percentages of urban and agricultural areas to most of our sample sites were very low (< 1%), there remains a possibility that point source inputs in urban or agricultural areas may also contribute to variability in DOM chemistry in our results.

Coniferous forest cover was common in all watersheds and dominated in most sites except for within the Connecticut watershed which was dominated by deciduous forest cover. Patterns of covariance among metrics of DOM diversity with % coniferous and % deciduous contributing forest cover were the most dynamic across watersheds of all the considered explanatory variables (Figs. S3 & S4). For example, DOM richness decreased significantly with increasing % coniferous forest cover in the Deschutes ($r = -0.78$) watershed while richness strongly increased with % coniferous forest cover in the Gunnison watershed ($r = 0.72$). Similarly, putative biochemical transformations decreased with increasing % coniferous forest cover in the Yakima ($r = -0.86$) and Deschutes ($r = -0.68$) watersheds while increasing in the Gunnison watershed ($r = 0.66$). The Connecticut watershed was the only watershed in this study with deciduous forest as a dominant land cover, although % deciduous forest cover in the Gunnison watershed sites ranged from 1 to 18%. A significant negative covariance was observed between DOM richness and % deciduous forest cover in the Connecticut watershed and the linear model for normalized transformations also decreased with increasing % deciduous cover although this model was not significant. While the mechanisms remain unclear, the observed negative covariance with % dominant

land cover in some watersheds is consistent with the positive covariance patterns observed with watershed area because the percentage of forest cover was typically greatest in headwater sites with smaller catchment areas. These results are also consistent with an earlier study conducted in the Yakima watershed at the same sites that found significant decreasing linear relations between putative biochemical transformations and increasing % forest land cover (Danczak et al. 2023).

While the direction of covariance between DOM diversity metrics and the proportion of dominant land cover is not conserved across watersheds, the significance of the relations suggest that the proportion of forest cover has a strong potential to coincide with watershed scale processes that drive DOM diversity. Despite the significant covariance observed with the land-use and land-cover explanatory variables in select watersheds, we reject hypotheses H4a and H4b because we did not find evidence of consistent patterns between DOM diversity metrics and land use explanatory variables that would allow for transferrable predictions across unsampled watersheds. These results further suggest that while land cover appears to be important for DOM diversity in all watersheds, the mechanisms underlying these connections likely vary across watersheds due to additional temporal and spatial factors (e.g., WRT) modulating the influence of land cover.

4 Conclusions

We explored relations among dependent variables that represent extractable DOM richness (e.g., number of assigned molecular formulas), composition (e.g., aromaticity index), and functional diversity (e.g., putative biochemical transformations) derived from FTICR-MS and explanatory variables associated with watershed characteristics (e.g., watershed area, surface-water residence time, land cover). While this study represents a significant sampling effort across a broad range of watershed characteristics in the United States, the results highlight both the continued challenges in generalizing interpretations that are applicable to all watersheds and the potential for overinterpreting studies that only consider a single watershed or watershed scale. The data presented here expand on many previous insightful investigations within smaller research watersheds (e.g., H.J. Andrews and Sleepers River; Silva et al. 2021; Wagner et al. 2019) where the development of conceptual frameworks is limited in transferability to Earth system models at larger spatial scales. The FTICR-MS results showed that the mass difference

684 analysis generating putative biochemical transformations displayed more consistent trends with
685 explanatory variables across watersheds than common bulk DOM parameters (e.g., DOC, aromaticity
686 index). Of all dependent variables, normalized putative biochemical transformations was the dependent
687 variable with the highest number of significant covariance across watersheds and explanatory variables
688 (n = 17). This study also found that the increasing DOM functional diversity pattern with watershed area
689 in the Yakima watershed was consistent across greater temporal resolution than previously reported by
690 Danczak et al. (2023). This congruence, and the detection of similar patterns in other similarly sized
691 watersheds in different ecological regions adds empirical evidence of trends in DOM diversity across
692 watershed scales that align with the resolution of Earth system models (100 - 10,000 km^2; Ward et al.
693 2020). The positive covariance of DOM composition and diversity with watershed area suggests relative
694 catchment position is associated with watershed processes that increase DOM diversity, although the
695 strength of this pattern is expected to vary among watersheds and may not be universally applicable.
696 We conclude that watershed area, WRT, and indices of temperature-dependent water column
697 reactivity (approximated by Da) are associated with mechanisms that increase DOM functional diversity
698 across basins (H1, H2, and H3) and that WRT in particular could be a universally applicable indicator of
699 the magnitude of DOM transformation along river flow paths. The concomitant increase in N-containing
700 DOM with these explanatory factors further supports the link between DOM composition and
701 biogeochemical reactivity across watersheds. Future studies that test the transferability of these patterns
702 across other similarly sized temperate watersheds are warranted. We also conclude that for some
703 watersheds, land use diversity is associated with increasing DOM diversity, but the potential mechanisms
704 underlying these relations may not be conserved across all watersheds. Future studies may build upon
705 these and other results to develop conceptual models predicting DOM diversity dynamics across large
706 watersheds of variable physiographic character. For example, assuming the dynamic range of normalized
707 putative biochemical transformations observed throughout a given watershed is an indicator of DOM
708 functional diversity, our results indicate that with each order of magnitude increase in watershed area,
709 relative DOM functional diversity could be expected to increase by 6 to 12% (± 3.7%). Similarly, the
710 linear-log model results indicate that relative DOM functional diversity increases by 5 to 22% (± 4.2%)
711 with each order of magnitude increase in surface WRT across similar sized watersheds. Furthermore, the

limitations of the number of samples available and the assessment of linear and linear-log covariance in this study inform considerations of future study design used to characterize nonlinear patterns within longitudinal gradients across watersheds. Future syntheses of DOM molecular properties that aim to ascertain generalizable patterns to inform Earth system models are likely to benefit from this public dataset and from additional analyses.

Statements and Declarations

Data availability

Dissolved organic carbon and raw FTICR-MS data was published in Torgeson et al. (2022) and Otenburg et al. (2022) in the ESS-DIVE repository and are licensed for reuse under the Creative Commons Attribution 4.0 International License.

Author Contributions

KAR, VAGC, BCC, TB, PAR and JCS conceptualized the study, VAGC processed FTICR-MS data and calculated biochemical transformations, KAR performed the analysis, TB, BCC, and PAR processed DOC samples. SL carried out the water residence time and dimensionless number calculations. KAR and VAGC drafted the initial manuscript and all authors contributed to revisions.

Competing interest

The authors declare no competing interests regarding this work.

Disclaimer

The authors have no relevant financial or non-financial interests to disclose. Any use of trade, firm, or product names is for descriptive purposes only and does not imply endorsement by the U.S. Government.

Funding

This study used data from the Worldwide Hydrobiogeochemistry Observation Network for Dynamic River Systems (WHONDRS). For this study, WHONDRS was supported by the River Corridor Science Focus Area (SFA) at the Pacific Northwest National Laboratory (PNNL). The SFA is supported by the United States Department of Energy, Office of Biological and Environmental Research (BER), Environmental System Science (ESS) Program. Some of the data used for this study were generated at the United States Department of Energy Environmental Molecular Science Laboratory User Facility. PNNL is operated by Battelle Memorial Institute for the United States Department of Energy under contract no. DE-AC05-76RL01830. Support was provided to P.A. Raymond and B.C. Crump by National Science Foundation award DEB-1840243. Support was provided to S. Liu by National Natural Science Foundation of China (52379057). We thank the United States Forest Service, Washington Department of Natural Resources, and Washington Department of Fish and Wildlife for access to field locations where these samples were collected.

References

Arora B, Briggs MA, Zarnetske JP, Stegen J, Gomez-Velez JD, Dwivedi D, Steefel C (2022) Hot Spots and Hot Moments in the Critical Zone: Identification of and Incorporation into Reactive Transport Models. In: Biogeochemistry of the Critical Zone. Advances in Critical Zone Science. p 9-47

Ball GI, Aluwihare LI (2014) CuO-oxidized dissolved organic matter (DOM) investigated with comprehensive two dimensional gas chromatography-time of flight-mass spectrometry (GC×GC-TOF-MS). Organic Geochemistry 75: 87-98

Bernhardt ES, Blaszczak JR, Ficken CD, Fork ML, Kaiser KE, Seybold EC (2017) Control Points in Ecosystems: Moving Beyond the Hot Spot Hot Moment Concept. Ecosystems 20(4): 665-682

Blodgett D, Johnson M (2022) D. Blodgett, M. Johnson, nhdplusTools: Tools for Accessing and Working with the NHDPlus (U.S. Geological Survey, 2022).

Bramer LM, White AM, Stratton KG, Thompson AM, Claborne D, Hofmockel K, McCue LA (2020) ftmsRanalysis: An R package for exploratory data analysis and interactive visualization of FT-MS data. PLoS Comput Biol 16(3): e1007654

Casas-Ruiz JP, Spencer RGM, Guillemette F, Schiller D, Obrador B, Podgorski DC, Kellerman AM, Hartmann J, Gómez-Gener L, Sabater S, Marcé R (2020) Delineating the Continuum of Dissolved Organic Matter in Temperate River Networks. Global Biogeochemical Cycles 34(8):

Coble AA, Wymore AS, Potter JD, McDowell WH (2022) Land Use Overrides Stream Order and Season in Driving Dissolved Organic Matter Dynamics Throughout the Year in a River Network. Environ Sci Technol 56(3): 2009-2020

Cole JJ, Prairie YT, Caraco NF, McDowell WH, Tranvik LJ, Striegl RG, Duarte CM, Kortelainen P, Downing JA, Middelburg JJ, Melack J (2007) Plumbing the Global Carbon Cycle: Integrating Inland Waters into the Terrestrial Carbon Budget. Ecosystems 10(1): 172-185

Cooper WT, Chanton JC, D'Andrilli J, Hodgkins SB, Podgorski DC, Stenson AC, Tfaily MM, Wilson RM (2022) A History of Molecular Level Analysis of Natural Organic Matter by FTICR Mass Spectrometry and The Paradigm Shift in Organic Geochemistry. Mass Spectrom Rev 41(2): 215-239

Creed IF, McKnight DM, Pellerin BA, Green MB, Bergamaschi BA, Aiken GR, Burns DA, Findlay SEG, Shanley JB, Striegl RG, Aulenbach BT, Clow DW, Laudon H, McGlynn BL, McGuire KJ, Smith RA, Stackpoole SM, Smith R (2015) The river as a chemostat: fresh perspectives on dissolved organic matter flowing down the river continuum. Canadian Journal of Fisheries and Aquatic Sciences 72(8): 1272-1285

Creed IF, Sanford SE, Beall FD, Molot LA, Dillon PJ (2003) Cryptic wetlands: integrating hidden wetlands in regression models of the export of dissolved organic carbon from forested landscapes. Hydrological Processes 17(18): 3629-3648

D'Andrilli J, Fischer SJ, Rosario-Ortiz FL (2020) Advancing Critical Applications of High Resolution Mass Spectrometry for DOM Assessments: Re-Engaging with Mass Spectral Principles, Limitations, and Data Analysis. Environ Sci Technol 54(19): 11654-11656

D'Andrilli J, Silverman V, Buckley S, Rosario-Ortiz FL (2022) Inferring Ecosystem Function from Dissolved Organic Matter Optical Properties: A Critical Review. Environ Sci Technol 56(16): 11146-11161

Danczak RE, Garayburu-Caruso VA, Renteria L, McKever SA, Otenburg OC, Grieger SR, Son K, Kaufman MH, Fulton SG, Roebuck JA, Myers-Pigg AN, Stegen JC (2023) Riverine organic matter functional diversity increases with catchment size. Frontiers in Water 5:

Dingman LS (2007) Analytical derivation of at-a-station hydraulic–geometry relations. Journal of Hydrology 334(1-2): 17-27

Dittmar T, Koch B, Hertkorn N, Kattner G (2008) A simple and efficient method for the solid-phase extraction of dissolved organic matter (SPE-DOM) from seawater. Limnol Oceanogr-Meth 6(6): 230-235

Dittmar T, Stubbins A (2014) Dissolved Organic Matter in Aquatic Systems. In: Treatise on Geochemistry. p 125-156

Garayburu-Caruso VA, Danczak RE, Stegen JC, Renteria L, McCall M, Goldman AE, Chu RK, Toyoda J, Resch CT, Torgeson JM, Wells J, Fansler S, Kumar S, Graham EB (2020) Using Community Science to Reveal the Global Chemogeography of River Metabolomes. Metabolites 10(12):

Gootman KS, González-Pinzón R, Knapp JLA, Garayburu-Caruso V, Cable JE (2020) Spatiotemporal Variability in Transport and Reactive Processes Across a First- to Fifth-Order Fluvial Network. Water Resources Research 56(5):

Harvey J, Gomez-Velez J, Schmadel N, Scott D, Boyer E, Alexander R, Eng K, Golden H, Kettner A, Konrad C, Moore R, Pizzuto J, Schwarz G, Soulsby C, Choi J (2019) How Hydrologic Connectivity Regulates Water Quality in River Corridors. J Am Water Resour Assoc 55(2): 369-381

Hawkes JA, D'Andrilli J, Agar JN, Barrow MP, Berg SM, Catalán N, Chen H, Chu RK, Cole RB, Dittmar T, Gavard R, Gleixner G, Hatcher PG, He C, Hess NJ, Hutchins RHS, Ijaz A, Jones HE, Kew W, Khaksari M, Palacio Lozano DC, Lv J, Mazzoleni LR, Noriega-Ortega BE, Osterholz H, Radoman N, Remucal CK, Schmitt ND, Schum SK, Shi Q, Simon C, Singer G, Sleighter RL, Stubbins A, Thomas MJ, Tolic N, Zhang S, Zito P, Podgorski DC (2020) An international laboratory comparison of dissolved organic matter composition by high resolution mass spectrometry: Are we getting the same answer? Limnology and Oceanography: Methods 18(6): 235-258

Hedges JI, Eglinton G, Hatcher PG, Kirchman DL, Arnosti C, Derenne S, Evershed RP, Kögel-Knabner I, de Leeuw JW, Littke R, Michaelis W, Rullkötter J (2000) The molecularly-uncharacterized component of nonliving organic matter in natural environments. Organic Geochemistry 31(10): 945-958

Hill RA, Weber MH, Leibowitz SG, Olsen AR, Thornbrugh DJ (2016) The Stream-Catchment (StreamCat) Dataset: A Database of Watershed Metrics for the Conterminous United States. JAWRA J. Am. Water Resour. Assoc. 52, 120–128. In.

Hockaday WC, Purcell JM, Marshall AG, Baldock JA, Hatcher PG (2009) Electrospray and photoionization mass spectrometry for the characterization of organic matter in natural waters: a qualitative assessment. Limnology and Oceanography: Methods 7(1): 81-95

Hosen JD, Aho KS, Fair JH, Kyzivat ED, Matt S, Morrison J, Stubbins A, Weber LC, Yoon B, Raymond PA (2020) Source Switching Maintains Dissolved Organic Matter Chemostasis Across Discharge Levels in a Large Temperate River Network. Ecosystems 24(2): 227-247

Hosen JD, Allen GH, Amatuli G, Breitmeyer S, Cohen MJ, Crump BC, Lu YH, Payet JP, Poulin BA, Stubbins A, Yoon B, Raymond PA (2021) River network travel time is correlated with dissolved organic matter composition in rivers of the contiguous United States. Hydrological Processes 35(5): 1-19

Inamdar S, Finger N, Singh S, Mitchell M, Levia D, Bais H, Scott D, McHale P (2012) Dissolved organic matter (DOM) concentration and quality in a forested mid-Atlantic watershed, USA. Biogeochemistry 108(1): 55-76

826 Johnson SL, Henshaw D, Downing G, Wondzell S, Schulze M, Kennedy A, Cohn G, Schmidt SA, Jones JA (2021) Long-term
827 hydrology and aquatic biogeochemistry data from H. J. Andrews Experimental Forest, Cascade Mountains, Oregon.
828 Hydrological Processes 35(5):
829 Kaplan LA, Cory RM (2016) Dissolved Organic Matter in Stream Ecosystems. In: Stream Ecosystems in a Changing
830 Environment. p 241-320
831 Kassambara A (2020) Package 'rstatix'. In. p Pipe-Friendly Framework for Basic Statistical Tests
832 Kim S, Kramer RW, Hatcher PG (2003) Graphical method for analysis of ultrahigh-resolution broadband mass spectra of
833 natural organic matter, the van Krevelen diagram. Anal Chem 75(20): 5336-5344
834 Koch BP, Dittmar T (2006) From mass to structure: an aromaticity index for high-resolution mass data of natural organic
835 matter. Rapid Communications in Mass Spectrometry 20(5): 926-932
836 Kujawinski EB, Hatcher PG, Freitas MA (2002) High-resolution Fourier transform ion cyclotron resonance mass spectrometry
837 of humic and fulvic acids: improvements and comparisons. Anal Chem 74(2): 413-419
838 Lauerwald R, Regnier P, Guenet B, Friedlingstein P, Ciais P (2020) How Simulations of the Land Carbon Sink Are Biased by
839 Ignoring Fluvial Carbon Transfers: A Case Study for the Amazon Basin. One Earth 3(2): 226-236
840 Lin P, Pan M, Allen GH, de Frasson RP, Zeng Z, Yamazaki D, Wood EF (2020) Global Estimates of Reach-Level Bankfull
841 River Width Leveraging Big Data Geospatial Analysis. Geophysical Research Letters 47(7):
842 Lin P, Pan M, Beck HE, Yang Y, Yamazaki D, Frasson R, David CH, Durand M, Pavelsky TM, Allen GH, Gleason CJ, Wood
843 EF (2019) Global Reconstruction of Naturalized River Flows at 2.94 Million Reaches. Water Resour Res 55(8): 6499-
844 6516
845 Liu S, Kuhn C, Amatulli G, Aho K, Butman DE, Allen GH, Lin P, Pan M, Yamazaki D, Brinkerhoff C, Gleason C, Xia X,
846 Raymond PA (2022a) The importance of hydrology in routing terrestrial carbon to the atmosphere via global streams
847 and rivers. Proc Natl Acad Sci U S A 119(11): e2106322119
848 Liu S, Maavara T, Brinkerhoff CB, Raymond PA (2022b) Global Controls on DOC Reaction Versus Export in Watersheds: A
849 Damköhler Number Analysis. Global Biogeochemical Cycles 36(4):
850 McClain ME, Boyer EW, Dent CL, Gergel SE, Grimm NB, Groffman PM, Hart SC, Harvey JW, Johnston CA, Mayorga E,
851 McDowell WH, Pinay G (2003) Biogeochemical Hot Spots and Hot Moments at the Interface of Terrestrial and
852 Aquatic Ecosystems. Ecosystems 6(4): 301-312
853 Mentges A, Feenders C, Seibt M, Blasius B, Dittmar T (2017) Functional Molecular Diversity of Marine Dissolved Organic
854 Matter Is Reduced during Degradation. Frontiers in Marine Science 4:
855 Messager ML, Lehner B, Grill G, Nedeva I, Schmitt O (2016) Estimating the volume and age of water stored in global lakes
856 using a geo-statistical approach. Nat Commun 7: 13603
857 Mosher JJ, Kaplan LA, Podgorski DC, McKenna AM, Marshall AG (2015) Longitudinal shifts in dissolved organic matter
858 chemogeography and chemodiversity within headwater streams: a river continuum reprise. Biogeochemistry 124(1-
859 3): 371-385
860 Otenburg O, Barnes M, Borton MA, Chen X, Chu R, Farris Y, Forbes B, Fulton SG, Garayburu-Caruso VA, Goldman AE,
861 Gonzalez BI, Grieger S, Kaufman MH, McKever SA, Myers-Pigg A, Pelly A, Renteria L, Scheibe TD, Son K,
862 Torgeson JM, Toyoda JG, Stegen JC (2022) Temporal Study 2021-2022: Sample-Based Surface Water Chemistry
863 and Organic Matter Characterization across Watersheds in the Yakima River Basin, Washington, USA (v2). River
864 Corridor and Watershed Biogeochemistry SFA, ESS-DIVE repository. Dataset. doi:10.15485/1898912. In.
865 Petchey OL, Gaston KJ (2006) Functional diversity: back to basics and looking forward. Ecol Lett 9(6): 741-758
866 Pielou EC (1966) The measurement of diversity in different types of biological collections. Journal of Theoretical Biology 13:
867 131-144
868 R Core Team (2023) R: A language and environment for statistical computing. In. R Foundation for Statistical Computing,
869 Vienna, Austria.
870 Raymond PA, Hartmann J, Lauerwald R, Sobek S, McDonald C, Hoover M, Butman D, Striegl R, Mayorga E, Humborg C,
871 Kortelainen P, Durr H, Meybeck M, Ciais P, Guth P (2013) Global carbon dioxide emissions from inland waters.
872 Nature 503(7476): 355-359
873 Raymond PA, Saiers JE, Sobczak WV (2016) Hydrological and biogeochemical controls on watershed dissolved organic
874 matter transport: pulse-shunt concept. Ecology 97(1): 5-16

875 Roebuck JA, Jr., Seidel M, Dittmar T, Jaffe R (2020) Controls of Land Use and the River Continuum Concept on Dissolved
876 Organic Matter Composition in an Anthropogenically Disturbed Subtropical Watershed. Environ Sci Technol 54(1):
877 195-206
878 Shanley JB, Sebestyen SD, McDonnell JJ, McGlynn BL, Dunne T (2015) Water's Way at Sleepers River watershed – revisiting
879 flow generation in a post-glacial landscape, Vermont USA. Hydrological Processes 29(16): 3447-3459
880 Silva MP, Blaurock K, Beudert B, Fleckenstein JH, Hopp L, Peiffer S, Reemtsma T, Lechtenfeld OJ (2021) Delineating Source
881 Contributions to Stream Dissolved Organic Matter Composition Under Baseflow Conditions in Forested Headwater
882 Catchments. Journal of Geophysical Research: Biogeosciences 126(8):
883 Spencer RGM, Butler KD, Aiken GR (2012) Dissolved organic carbon and chromophoric dissolved organic matter properties
884 of rivers in the USA. Journal of Geophysical Research: Biogeosciences 117(G3): G03001
885 Stadler M, Barnard MA, Bice K, de Melo ML, Dwivedi D, Freeman EC, Garayburu-Caruso VA, Linkhorst A, Mateus-Barros
886 E, Shi C, Tanentzap AJ, Meile C (2023) Applying the core-satellite species concept: Characteristics of rare and
887 common riverine dissolved organic matter. Frontiers in Water 5:
888 Stegen JC, Fansler SJ, Tfaily MM, Garayburu-Caruso VA, Goldman AE, Danczak RE, Chu RK, Renteria L, Tagestad J,
889 Toyoda J (2022) Organic matter transformations are disconnected between surface water and the hyporheic zone.
890 Biogeosciences 19(12): 3099-3110
891 Stegen JC, Johnson T, Fredrickson JK, Wilkins MJ, Konopka AE, Nelson WC, Arntzen EV, Chrisler WB, Chu RK, Fansler
892 SJ, Graham EB, Kennedy DW, Resch CT, Tfaily M, Zachara J (2018) Influences of organic carbon speciation on
893 hyporheic corridor biogeochemistry and microbial ecology. Nat Commun 9(1): 585
894 Tanentzap AJ, Fitch A, Orland C, Emilson EJS, Yakimovich KM, Osterholz H, Dittmar T (2019) Chemical and microbial
895 diversity covary in fresh water to influence ecosystem functioning. Proc Natl Acad Sci U S A:
896 Tank JL, Rosi-Marshall EJ, Griffiths NA, Entrekin SA, Stephen ML (2010) A review of allochthonous organic matter
897 dynamics and metabolism in streams. Journal of the North American Benthological Society 29(1): 118-146
898 Torgeson JM, Bambakidis T, Bates TL, Chu R, Crump BC, R.E. D, B. F, V.A. G-C, A.E. G, L. L, T. M, E.W. M, S.A. M, B.
899 P-M, P.A. R, L. R, J.G. T, J.C. S (2022) WHONDRS Surface Water Dissolved Organic Carbon and FTICR-MS across
900 Stream Orders in Four United States Watersheds in 2019 and 2020. River Corridor and Watershed Biogeochemistry
901 SFA, ESS-DIVE repository. Dataset. doi:10.15485/1895159 In.
902 Tranvik LJ, Cole JJ, Prairie YT (2018) The study of carbon in inland waters—from isolated ecosystems to players in the global
903 carbon cycle. Limnology and Oceanography Letters 3(3): 41-48
904 U.S. Geological Survey (2016) National Water Information System data available on the World Wide Web (USGS Water Data
905 for the Nation), accessed January 20, 2023, at URL http://waterdata.usgs.gov/nwis/. In.
906 Vannote RL, Minshall GW, Cummins KW, Sedell JR, Cushing CE (1980) The River Continuum Concept. Canadian Journal
907 of Fisheries and Aquatic Sciences 37(1): 130-137
908 Vano JA, Scott MJ, Voisin N, Stöckle CO, Hamlet AF, Mickelson KEB, Elsner MM, Lettenmaier DP (2010) Climate change
909 impacts on water management and irrigated agriculture in the Yakima River Basin, Washington, USA. Climatic
910 Change 102(1-2): 287-317
911 Vaughn DR, Kellerman AM, Wickland KP, Striegl RG, Podgorski DC, Hawkings JR, Nienhuis JH, Dornblaser MM, Stets
912 EG, Spencer RGM (2021) Anthropogenic landcover impacts fluvial dissolved organic matter composition in the
913 Upper Mississippi River Basin. Biogeochemistry:
914 Vaughn DR, Kellerman AM, Wickland KP, Striegl RG, Podgorski DC, Hawkings JR, Nienhuis JH, Dornblaser MM, Stets
915 EG, Spencer RGM (2023) Bioavailability of dissolved organic matter varies with anthropogenic landcover in the
916 Upper Mississippi River Basin. Water Res 229: 119357
917 Wagner S, Fair JH, Matt S, Hosen JD, Raymond P, Saiers J, Shanley JB, Dittmar T, Stubbins A (2019) Molecular Hysteresis:
918 Hydrologically Driven Changes in Riverine Dissolved Organic Matter Chemistry During a Storm Event. Journal of
919 Geophysical Research: Biogeosciences 124(4): 759-774
920 Wagner S, Riedel T, Niggemann J, Vahatalo AV, Dittmar T, Jaffe R (2015) Linking the Molecular Signature of Heteroatomic
921 Dissolved Organic Matter to Watershed Characteristics in World Rivers. Environ Sci Technol 49(23): 13798-13806
922 Ward ND, Megonigal JP, Bond-Lamberty B, Bailey VL, Butman D, Canuel EA, Diefenderfer H, Ganju NK, Goni MA, Graham
923 EB, Hopkinson CS, Khangaonkar T, Langley JA, McDowell NG, Myers-Pigg AN, Neumann RB, Osburn CL, Price
924 RM, Rowland J, Sengupta A, Simard M, Thornton PE, Tzortziou M, Vargas R, Weisenhorn PB, Windham-Myers L

(2020) Representing the function and sensitivity of coastal interfaces in Earth system models. Nat Commun 11(1): 2458

Willi K, Ross MRV (2023) Geospatial Data Puller for Waters in the Contiguous United States (Version v1). Zenodo data release, DOI: 10.5281/zenodo.8140272. In.

Wollheim WM, Bernal S, Burns DA, Czuba JA, Driscoll CT, Hansen AT, Hensley RT, Hosen JD, Inamdar SP, Kaushal SS, Koenig LE, Lu YH, Marzadri A, Raymond PA, Scott D, Stewart RJ, Vidon PG, Wohl E (2018) River network saturation concept: factors influencing the balance of biogeochemical supply and demand of river networks. Biogeochemistry 141(3): 503-521

Wollheim WM, Stewart RJ, Aiken GR, Butler KD, Morse NB, Salisbury J (2015) Removal of terrestrial DOC in aquatic ecosystems of a temperate river network. Geophysical Research Letters 42(16): 6671-6679

Xenopoulos MA, Barnes RT, Boodoo KS, Butman D, Catalán N, D'Amario SC, Fasching C, Kothawala DN, Pisani O, Solomon CT, Spencer RGM, Williams CJ, Wilson HF (2021) How humans alter dissolved organic matter composition in freshwater: relevance for the Earth's biogeochemistry. Biogeochemistry 154(2): 323-348

Yoon B, Hosen JD, Kyzivat ED, Fair JH, Weber LC, Aho KS, Lowenthal R, Matt S, Sobczak WV, Shanley JB, Morrison J, Saiers JE, Stubbins A, Raymond PA (2021) Export of photolabile and photoprimable dissolved organic carbon from the Connecticut River. Aquatic Sciences 83(2):

Zarnetske JP, Haggerty R, Wondzell SM, Bokil VA, González-Pinzón R (2012) Coupled transport and reaction kinetics control the nitrate source-sink function of hyporheic zones. Water Resources Research 48(11):

Supplemental Information for:

Riverine dissolved organic matter transformations increase with watershed area, water residence time, and Damköhler numbers in nested watersheds

Kevin A. Ryan[1*], Vanessa A. Garayburu-Caruso[2*], Byron C. Crump[3], Ted Bambakidis[3], Peter A. Raymond[4], Shaoda Liu[5], James C. Stegen[2,6]

[1]U.S. Geological Survey New York Water Science Center, Troy, New York, USA, 12180
[2]Pacific Northwest National Laboratory, Richland, Washington, USA, 99354
[3]Oregon State University, Corvallis, Oregon, USA, 97331
[4]Yale University, New Haven, Connecticut, USA, 06511
[5]School of Environment, Beijing Normal University, Beijing, China, 100875
[6] Washington State University, Pullman, WA 99163

Correspondence to: Kevin A. Ryan (karyan@usgs.gov)

Summary:

This supplement provides a table of sampling locations and watershed attributes and figures displaying results of dissolved organic matter chemistry (i.e., dependent variables) across watersheds (Fig. S1), seasons (Fig. S2), % coniferous land cover (Fig. S3), and % deciduous land cover (Fig. S4).

Table S1. Characteristics of study sites in the United States including watershed, site, mean elevation (m, datum = NAVD88), stream order, watershed area (km^2), dimensionless stream slope, and percent of contributing area land classification for water (% Wat.), developed (% Dev.), barren (% Bar.), forest (% Forest), ice and snow (% Ice_snow), grassland (% Grass.), shrubland (%Shrub.), agriculture (% Ag.), and wetland (% Wet.). Data are sourced from Blodgett and Johnson (2022) and Hill et al. (2016). CT = Connecticut River, Connecticut; DES = Deschutes River, Oregon; GUN = Gunnison River watershed, Colorado; WIL = Willamette River, Oregon; YRB = Yakima River Basin, Washington state.

Watershed	Site	Elevation, m	Stream Order	Area	Stream slope	% Wat.	% Dev.	% Bar.	% Forest	% Ice_snow	% Grass.	% Shrub.	% Ag.	% Wet.
CT	CT-BUNN	281	1	10.5	0.0112	0.4	14.4	0	64.1	0	1	0.3	9.5	10.2
CT	CT-EBRA	518	3	139.3	0.0046	0.7	3.4	0	87.8	0	0.8	1.5	1	4.8
CT	CT-FARM	273	5	1492.9	0.0028	2.9	16.2	0.2	68	0	0.5	0.5	3.3	8.4
CT	CT-MOOS	536	3	208.9	0.007	0.1	1.8	0	89.1	0	0.6	1.6	0.2	6.7
CT	CT-NEPA	257	3	62.1	0.0009	0.3	9.8	0	75.1	0	0.5	0.8	6.2	7.3
CT	CT-PASS	440	4	1125.1	0.0066	0.4	6.5	0.1	77.9	0	0.6	2.1	8.2	4.3
CT	CT-PHEL	246	1	7.8	0.0207	0.3	9.6	0	70.1	0	1.6	0.5	4.3	13.7
CT	CT-POPE	492	1	11.1	0.0385	0	4.2	0	78.2	0	0.2	2.2	14	1.1
CT	CT-SLPR	402	3	120.5	0.0067	0	6.8	0.1	73.7	0	0.4	2.2	14	2.8
CT	CT-STIL	368	4	222.7	0.0057	2.3	9.8	0.2	76	0	0.4	0.3	2.4	8.7
CT	CT-THOM	384	6	25009	0.0006	1.9	8	0.2	76.6	0	0.6	1.5	5.6	5.6
CT	CT-UNIO	340	5	978.6	0	3.8	8.4	0.2	76.3	0	0.5	0.6	2	8.2
CT	CT-W9	570	1	0.41	0.206	0	0	0	100	0	0	0	0	0
DES	BRO-LAP	1575	2	51.9	0.0054	0.3	1.5	0.1	93.6	0	0.3	2.9	0	1.4
DES	CUL-LAP	1561	2	52	0.0018	0.7	0.6	0.4	94.6	0	0.2	3.1	0	0.4
DES	DES-BFA	1496	5	3606.9	0.0005	2.1	2.6	0.3	70.5	0	2.6	19	0.2	2.7
DES	DES-LAP	1605	2	106.6	0.0038	1.9	1.9	2.1	84.2	0	1.8	6.5	0	1.7
DES	DES-MAD	1314	6	18388	0.0029	0.7	2.7	0.6	31.6	0.1	5.1	55	2.8	1.4
DES	DES-MOO	1194	6	25189	0.0027	0.6	2.3	0.5	29.3	0.1	15.1	47.4	3.8	1.1
DES	DES-WIC	1523	4	662.4	0.0076	5.9	0.9	0.5	82.9	0	1	5.6	0	3.3
DES	LDS-LAP	1499	4	1862.2	0.0004	1	2	0.2	65.8	0	2.4	25.6	0.2	2.9
DES	TRO-GAT	1002	5	1668.3	0.0088	0	0.9	0	12.5	0	37.8	43.9	4.8	0.1
DES	WHY-SIS	1709	3	166.3	0.0114	0.1	0.5	17.3	33.2	3.2	26.9	18.1	0.3	0.3
GUN	EAS-ALM	3131	4	749.4	0.0086	0.1	1.9	3.3	48	0.5	4.3	34.3	1.3	6.4
GUN	EAS-BRA	3507	1	4.9	0.1294	0	0.3	23.7	33.9	2.4	7.2	29	0	3.6
GUN	EAS-PUM	3335	2	86.7	0.0135	0.1	1.2	11	34.2	2.5	6.1	37.4	0	7.5
GUN	EAS-ROC	3358	1	4.6	0.1524	0	0.4	2.8	57.2	0.1	5.6	30	0	4

GUN	EAS-RUS	3483	1	15	0.1043	0	0	11.9	20.3	2.7	13.5	40.6	0	11
GUN	GUN-GRJ	2668	6	20482	0	0.4	1.4	2.3	53.2	0	4.3	31.9	4.4	2.1
GUN	GUN-GUN	3106	5	2645.9	0.0085	0.4	1.2	2.3	53.7	0.3	3.6	31.5	2	5.1
GUN	GUN-R32	3027	6	5509.4	0.0065	0.2	0.9	1.6	50.7	0.1	4.1	36.4	2	4
GUN	GUN-TUN	3009	6	10284	0	0.5	0.7	2.9	52.2	0.1	6.6	32.7	1.3	3
GUN	TAY-RES	3314	5	662.7	0.0264	1.2	0.4	4.2	56.4	0.4	5.2	25	0	7.2
GUN	TAY-TAY	3329	4	331.3	0.0142	0.1	0	4.3	54.9	0.4	5.2	26.6	0	8.5
WIL	BLU-BLU	929	4	228	0.0412	1.2	0.2	0.2	95.2	0	0.3	3	0	0
WIL	BLU-TID	974	3	119.4	0.007	0	0	0	95.9	0	0.3	3.8	0	0
WIL	LOO-BLU	980	3	63.6	0.0205	0	0	0	98.5	0	0.1	1.4	0	0
WIL	MCK-WAL	1078	5	2730.9	0.0011	0.6	0.9	3.3	83.8	0.2	5.8	4.9	0.3	0.3
WIL	WIL-COR	725	6	11376	0.0003	1.3	4.3	0.9	71.4	0.1	3.1	5.5	12.1	1.5
WIL	WIL-GOS	598	5	1664.3	0.0013	0.6	3.1	0	75.8	0	4	8	7.4	1.1
WIL	WIL-HAR	881	6	8825.8	0.0009	1.2	2.6	1.1	80.8	0.1	3.5	6.1	3.9	0.8
WIL	WIL-JAS	1006	5	3494.9	0.009	1.9	0.9	0.3	87.7	0	1.5	6.2	1.4	0.3
WIL	WIL-POR	555	7	28922	0	1	8.1	0.4	59.8	0	2.6	5.3	20.9	1.7
WIL	HJA-WS2	812	1	0.6	0.5319	0	0	0	100	0	0	0	0	0
WIL	HJA-WS1	733	1	0.96	0.5935	0	0	0	100	0	0	0	0	0
YRB	T02	905	7	13462	0.0004	0.7	5.2	0.6	32.6	0.1	23.7	22.2	13.4	1.5
YRB	T03	1030	7	8977.1	0.0008	0.9	5.4	0.9	41.6	0.1	17.4	24.5	8.3	1
YRB	T05P	1311	4	383.9	0.0056	0.1	2.1	0.2	78.2	0	13.1	5.6	0	0.8
YRB	T06	1464	3	206.2	0.0173	0.2	0.8	1	65.7	0	22.3	8.4	0.2	1.4
YRB	T07	880	7	14145	0.0017	0.7	5.5	0.6	31.1	0.1	23.6	22.3	14.8	1.5
YRB	T41	1315	6	2465.9	0.006	0.9	2.8	1.5	70.9	0.2	8.9	13.5	0.4	1.1
YRB	T42	1315	6	2465.9	0.006	0.9	2.8	1.5	70.9	0.2	8.9	13.5	0.4	1.1

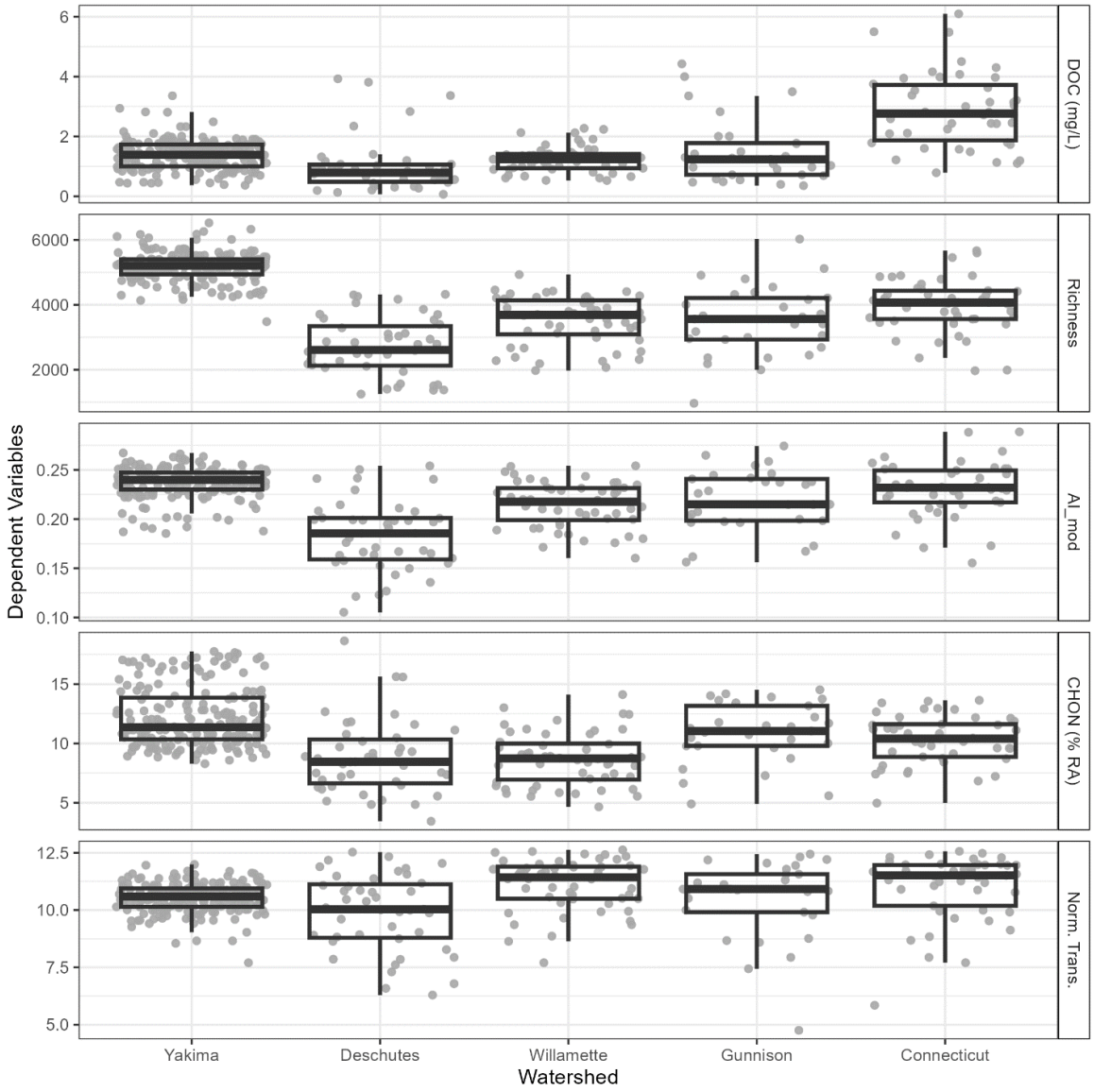

Figure S1. Boxplot of dependent variables versus watershed for five watersheds in the United States. Y-axis variables are dissolved organic carbon (DOC) concentration, number of assigned formulas (Richness), modified aromaticity index (AI_mod), the percent relative abundance of assigned molecular formula containing carbon, hydrogen, oxygen, and nitrogen (C, H, O, and N) normalized to the total number of formula (CHON, % RA), and the total number of putative biochemical transformations normalized by number of assigned formulas (Norm. Trans.). Box plots depict the median and first and third quartiles. Whiskers extend to the minimum or maximum value no further than 1.5 times the inner quartile range. Grey points depict all of the data used to generate the box plots. Connecticut = Connecticut River, Connecticut; Deschutes River, Oregon; Gunnison River watershed, Colorado; Willamette River, Oregon; Yakima River Basin. Washington state.

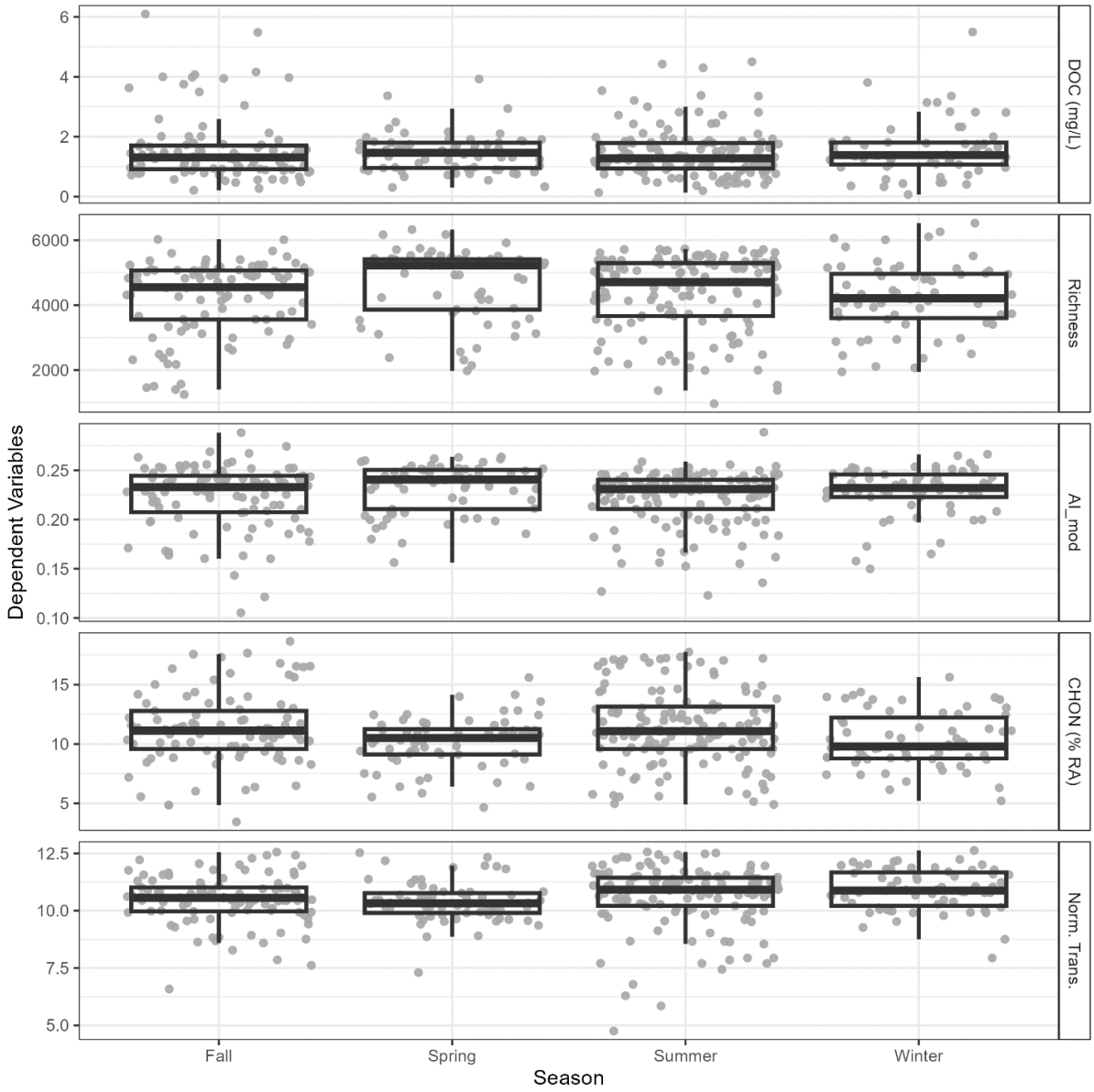

Figure S2. Boxplot of dependent variables versus season for five watersheds in the United States. Y-axis variables are dissolved organic carbon (DOC) concentration, number of assigned formulas (Richness), modified aromaticity index (AI_mod), the percent relative abundance of assigned molecular formula containing carbon, hydrogen, oxygen, and nitrogen (C, H, O, and N) normalized to the total number of formula (CHON, % RA), and the total number of putative biochemical transformations normalized by number of assigned formulas (Norm. Trans.). Box plots depict the median and first and third quartiles. Whiskers extend to the minimum or maximum value no further than 1.5 times the inner quartile range. Grey points depict all of the data used to generate the box plots.

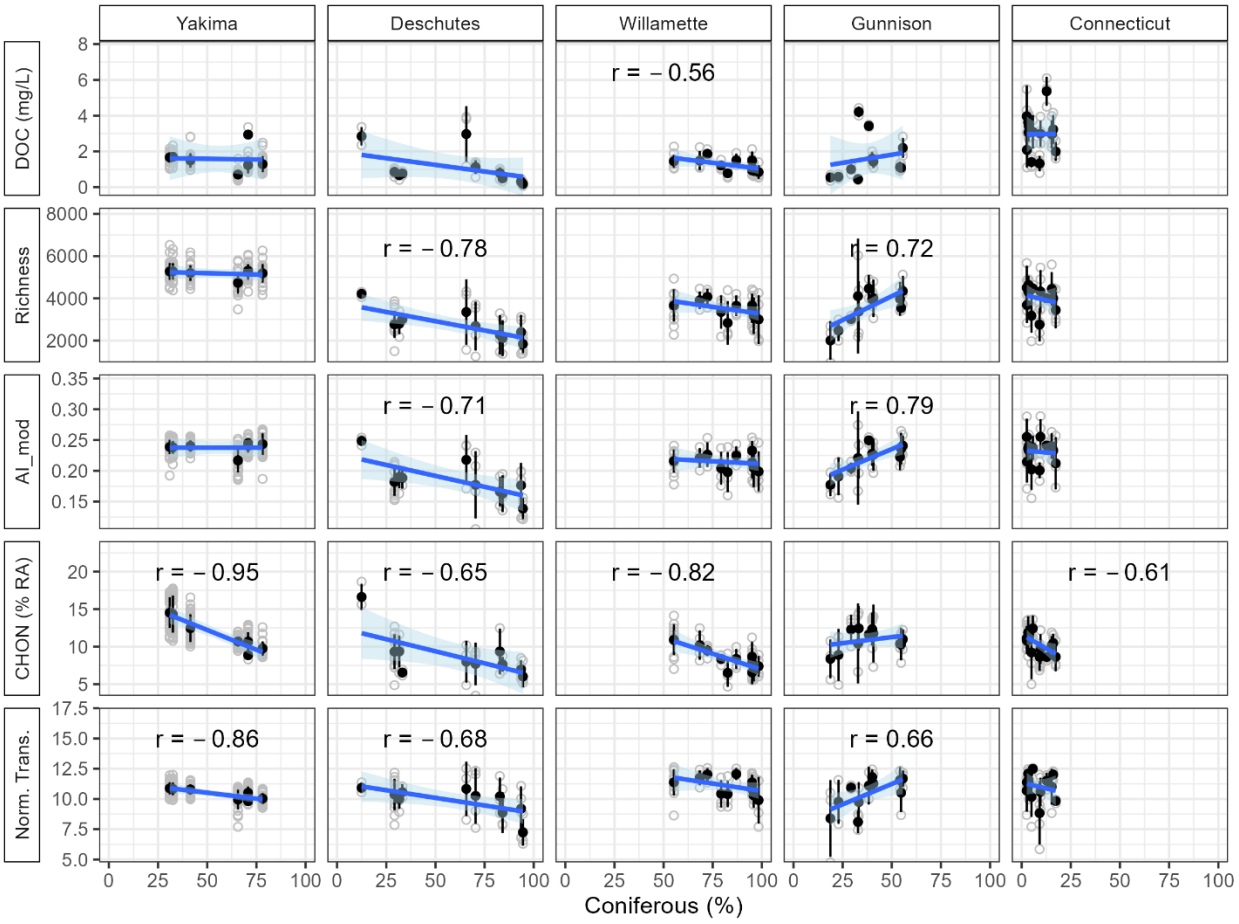

Figure S3. Dependent variables dissolved organic carbon (DOC) concentration, number of assigned formulas (Richness), modified aromaticity index (AI_mod), the percent relative abundance of assigned molecular formula containing carbon, hydrogen, oxygen, and nitrogen (C, H, O, and N) normalized to the total number of formula (CHON, % RA), and the total number of putative biochemical transformations normalized by number of assigned formulas (Norm. Trans.) versus percent coniferous land cover for each of five watersheds in the United States. Solid black points and error bars represent the mean and standard deviation of a sample site. Open grey circles represent all data. Linear regression line of best fit is shown in blue and 95% confidence interval is shown in light blue. Correlation coefficients (r) are shown when $p < 0.1$.

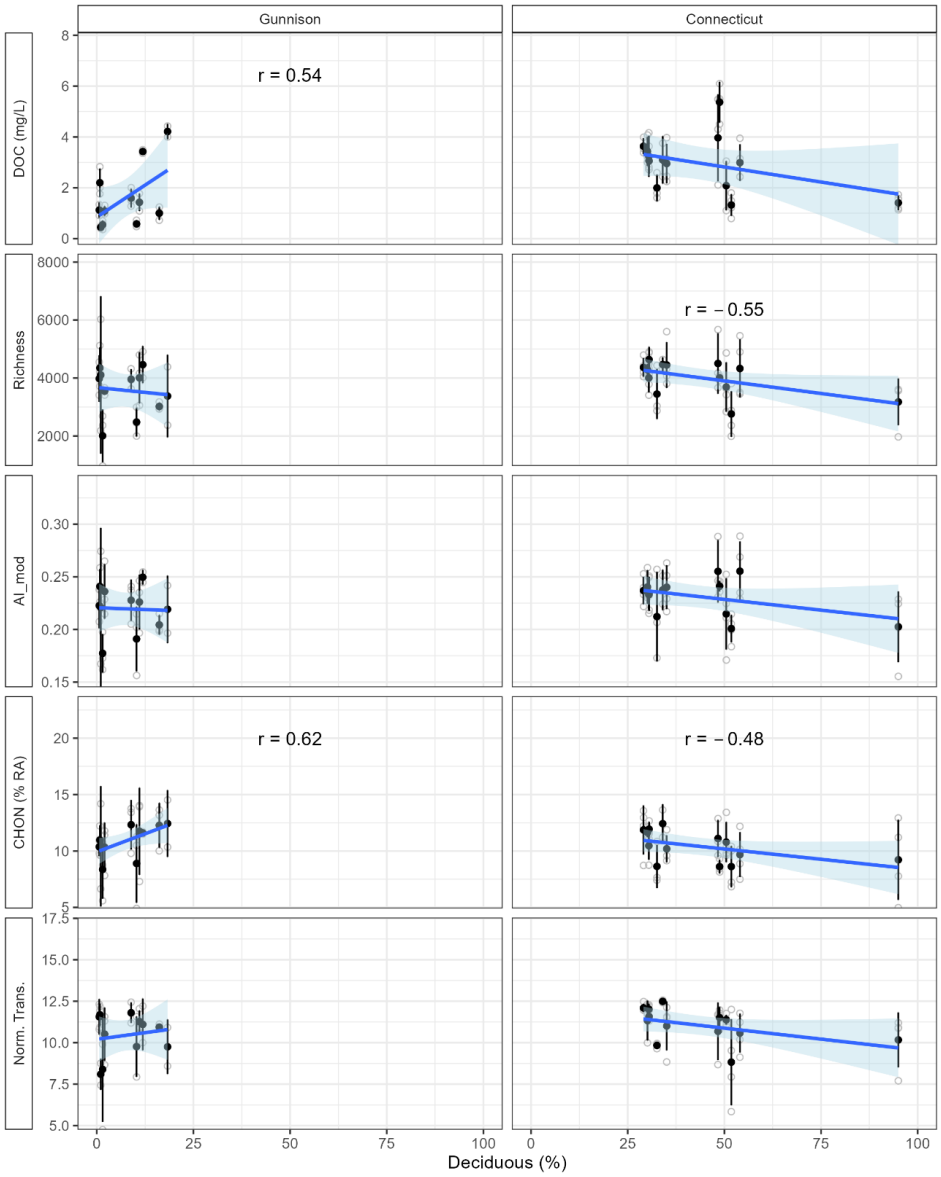

Figure S4. Dependent variables dissolved organic carbon (DOC) concentration, number of assigned formulas (Richness), modified aromaticity index (AI_mod), the percent relative abundance of assigned molecular formula containing carbon, hydrogen, oxygen, and nitrogen (C, H, O, and N) normalized to the total number of formula (CHON, % RA), and the total number of putative biochemical transformations normalized by number of assigned formulas (Norm. Trans.) versus percent deciduous land cover for each of two watersheds (Gunnison River, Connecticut River) in the United States. Solid black points and error bars represent the mean and standard deviation of a sample site. Open grey circles represent all data. Linear regression line of best fit is shown in blue and 95% confidence interval is shown in light blue. Correlation coefficients (r) are shown when $p < 0.1$.

Supplemental References

Blodgett D, Johnson M (2022) D. Blodgett, M. Johnson, nhdplusTools: Tools for Accessing and Working with the NHDPlus (U.S. Geological Survey, 2022).

Hill RA, Weber MH, Leibowitz SG, Olsen AR, Thornbrugh DJ (2016) The Stream-Catchment (StreamCat) Dataset: A Database of Watershed Metrics for the Conterminous United States. JAWRA J. Am. Water Resour. Assoc. 52, 120–128. In.